The phase-space structure of primordial halos: Vlasov simulations of 3 crossed sine waves

S. Colombi (Institut d'Astrophysique de Paris)

Colombi 2015, MNRAS 446, 2902
Sousbie & Colombi 2016, JCP 321, 644
Taruya & Colombi 2017, MNRAS 470, 4858
Saga, Taruya & Colombi 2018, arXiv:1805.08787
Colombi et al. 2018, in prep.

Plan

- Vlasov-Poisson equations and the mean-field limit
- Limits of *N*-body simulation techniques
- Direct solver: the cold case
- Structure of a proto-halo: collapse and post-collapse

Stars in galaxies, dark matter in the Universe: large ensembles of many particles interacting with each other through gravitational force

Microscopic level: dynamics of an ensemble of particles: Campa, Dauxois & Ruffo 2009, Phys. Rep. 480, 57

(θ, p) Eulerian coordinates in phase-space

(Θ_i, P_i) Lagrangian coordinates in phase-space: positions and velocities

Lagrangian equations of motion

$$\dot{\Theta}_j = P_j,$$
$$\dot{P}_j = -\frac{\partial U}{\partial \Theta_j}.$$

$$U(\Theta_1, \ldots, \Theta_N) = \sum_{i<j}^{N} V(\Theta_i - \Theta_j)$$ Gravitational potential

Phase-space density: $$f_d(\theta, p, t) = \frac{1}{N} \sum_{j=1}^{N} \delta\left(\theta - \Theta_j(t)\right) \delta\left(p - P_j(t)\right)$$

Klimontovich equation:

$$\boxed{\frac{\partial f_d}{\partial t} + p\frac{\partial f_d}{\partial \theta} - \frac{\partial v}{\partial \theta}\frac{\partial f_d}{\partial p} = 0}$$

with $$v(\theta, t) = N \int \mathrm{d}\theta' \mathrm{d}p' V(\theta - \theta') f_d(\theta', p', t)$$

Macroscopic level: average behaviour over many realisations

Phase-space density is now the result of the ensemble average over the states obtained from over many initial conditions with a given initial density probability $f_{\rm in}(\{\Theta_i(0), P_i(0)\})$

$$f_0(\theta, p, t) \equiv \langle f_d(\theta, p, t)\rangle = \int \prod_i \mathrm{d}\Theta_i(0)\mathrm{d}P_i(0) f_{\rm in}(\{\Theta_i(0), P_i(0)\}) f_d(\theta, p, t)$$

A given realisation is a fluctuation around the mean:

$$f_d(\theta, p, t) = f_0(\theta, p, t) + \frac{1}{\sqrt{N}}\delta f(\theta, p, t) \qquad v(\theta, t) = \langle v\rangle(\theta, t) + \frac{1}{\sqrt{N}}\delta v(\theta, t)$$

Average potential: $\langle v\rangle(\theta, t) = N\int \mathrm{d}\theta'\mathrm{d}p' V(\theta - \theta') f_0(\theta', p', t)$

$$\frac{\partial f_0}{\partial t} + p\frac{\partial f_0}{\partial \theta} - \frac{\partial \langle v\rangle}{\partial \theta}\frac{\partial f_0}{\partial p} = \frac{1}{N}\left\langle \frac{\partial \delta v}{\partial \theta}\frac{\partial \delta f}{\partial p}\right\rangle$$

First moment of BBGKY hierarchy

$N \to \infty$

This limit is not yet fully demonstrated for Gravitational force in 3D !

(e.g. Jabin & Wang 2017, Active Particles, Volume 1, 379)

$$\frac{\partial f_0}{\partial t} + p\frac{\partial f_0}{\partial \theta} - \frac{\partial \langle v\rangle}{\partial \theta}\frac{\partial f_0}{\partial p} = 0$$

Vlasov (Collisionless Bolztmann) equation

Hénon 1982, A&A 114, 211

Simulations techniques : the N-body approach

- System modelled by an ensemble of macro-particles obeying the Lagrangian equations of motion, each of them representing many micro-particles: *we come back to Klimontovich !*

Phase-space position (**r**,**u**)

$$\mathrm{d}\mathbf{r}/\mathrm{d}t = \mathbf{u},$$

$$\mathrm{d}\mathbf{u}/\mathrm{d}t = \mathbf{a} = -\nabla\phi$$

- A softening **ε** of the force is introduced at small scales to avoid catastrophic behaviour

- All the codes basically differ by the way Poisson equation is solved

$$\Delta_{\mathbf{r}}\phi = 4\pi G\rho = 4\pi G \int f(\mathbf{r}, \mathbf{u}, t)\, \mathrm{d}^3\mathbf{u}$$

Issues: macroscopic versus microscopic

(beyond approximations used to speed up solving Poisson equation and resolve equations of motion)

- The true system might follow closely the large-*N* limit (Vlasov) while the simulated one does not: this is particularly true for dark matter
- How to disentangle numerical instabilities due to *N* “not large enough” from true physical instabilities in the system?
- What are the consequences of modifying the actual interaction potential with a softening? How large should be the softening?
- How difficult is it, actually, to simulate systems with cold initial conditions?

Vlasov versus *N*-body

Example: phase-space of a 1D simulation with Gaussian initial conditions

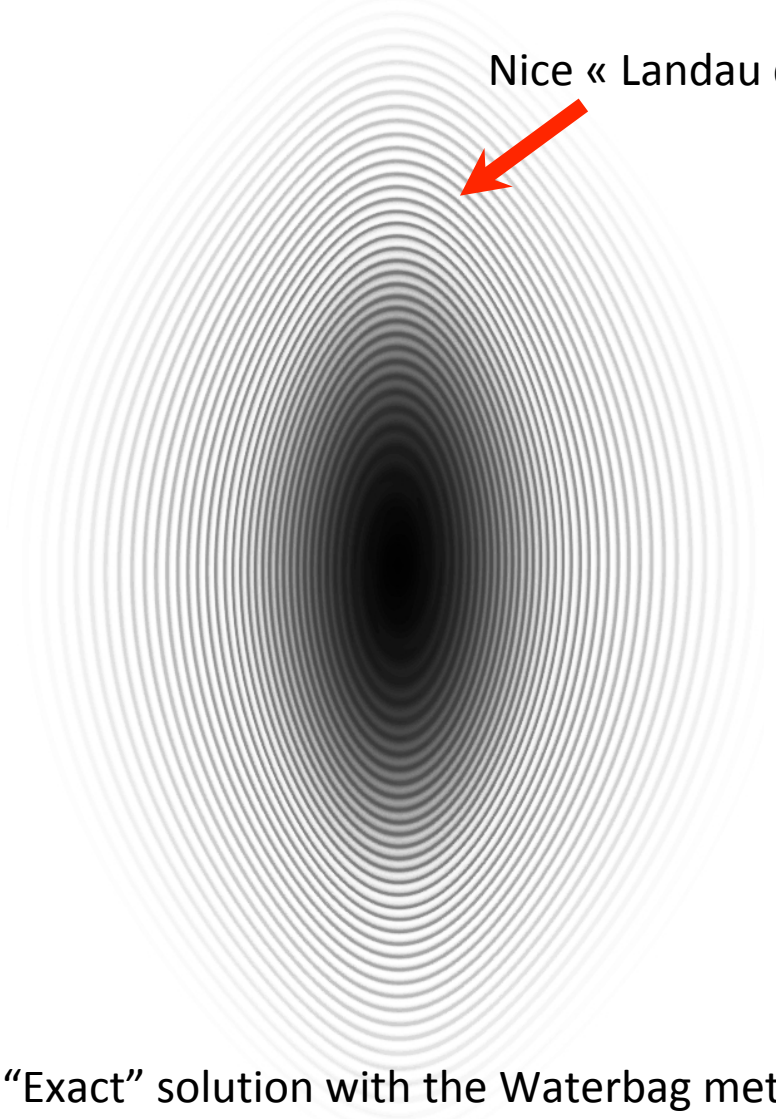

"Exact" solution with the Waterbag method

Colombi & Touma (2008, 2014)

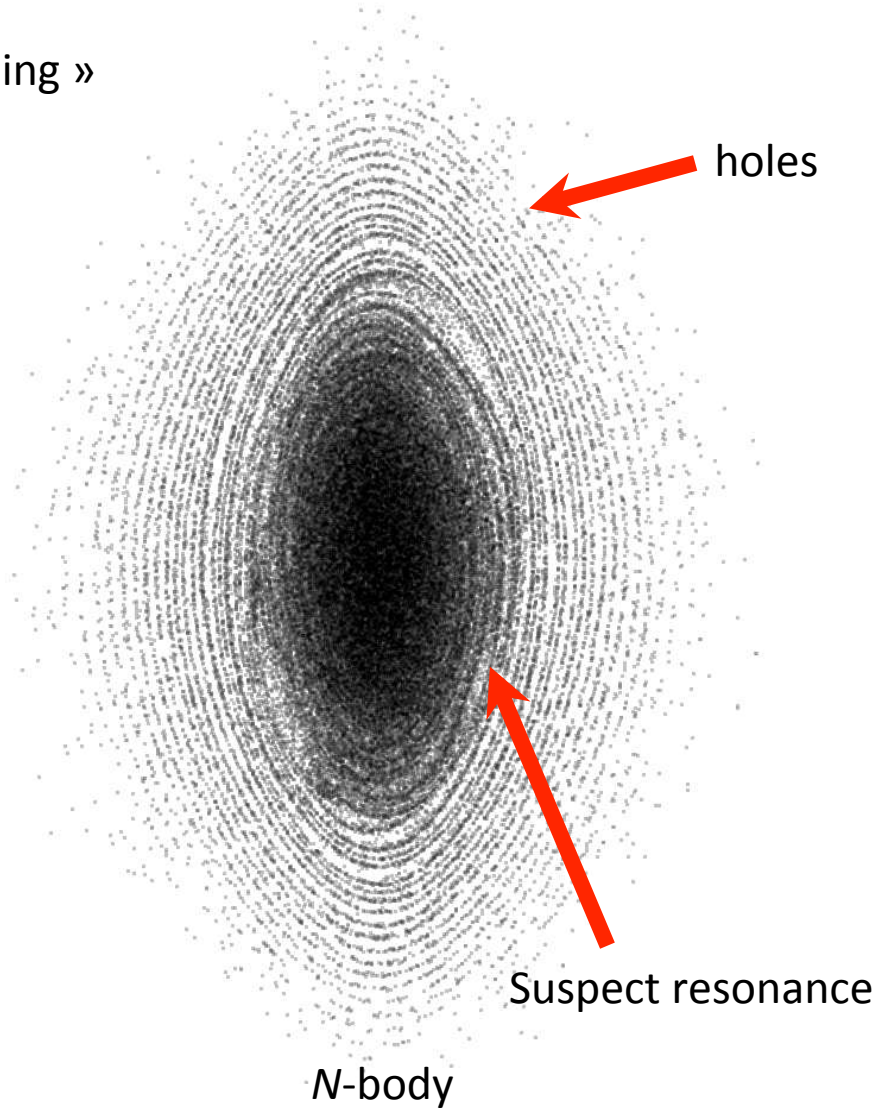

N-body

Test particles in a 2D Plummer potential

Image : T. Sousbie

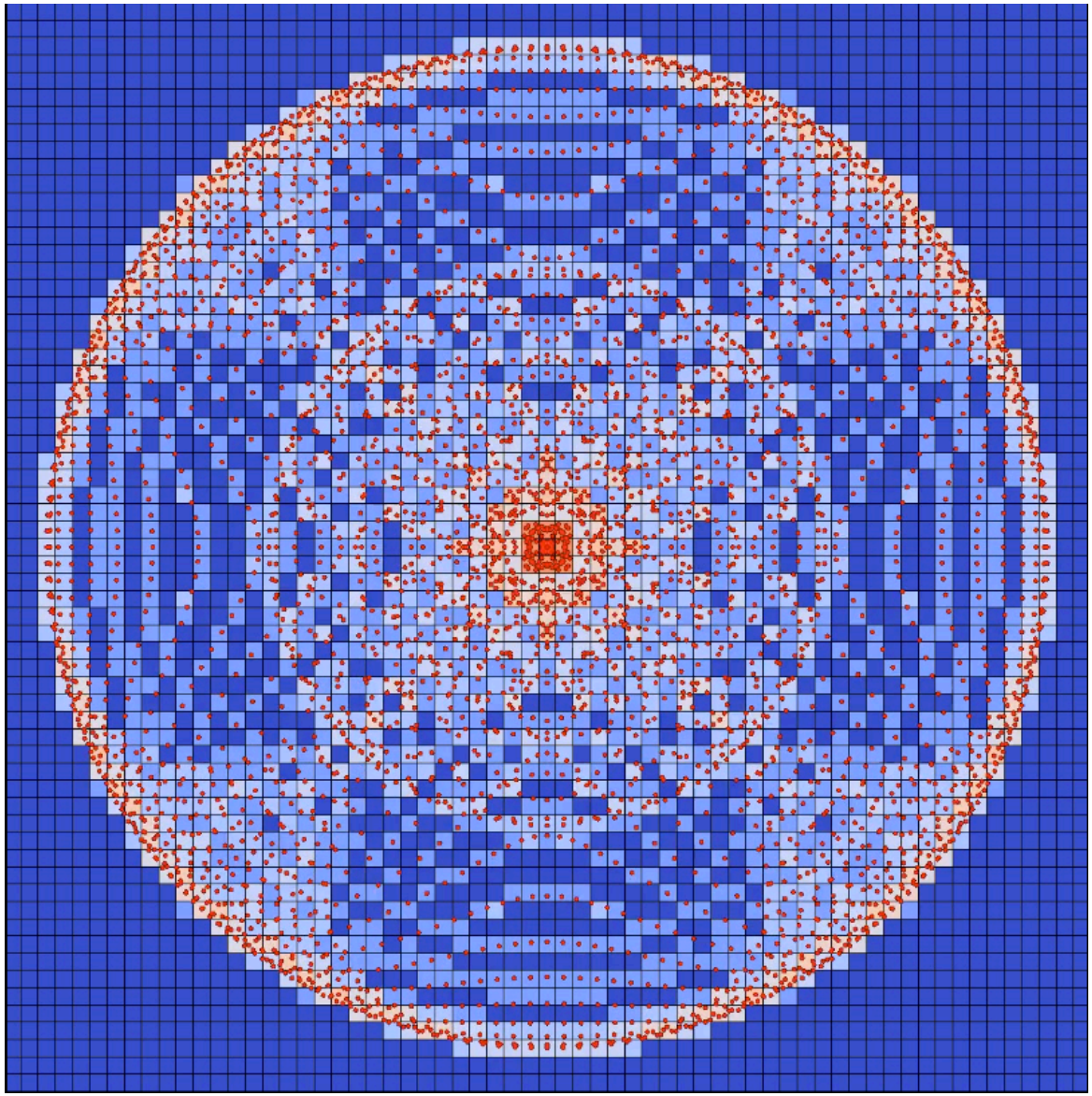

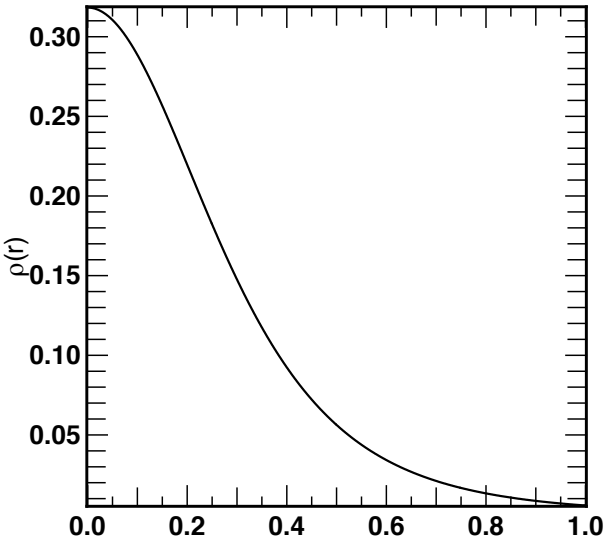

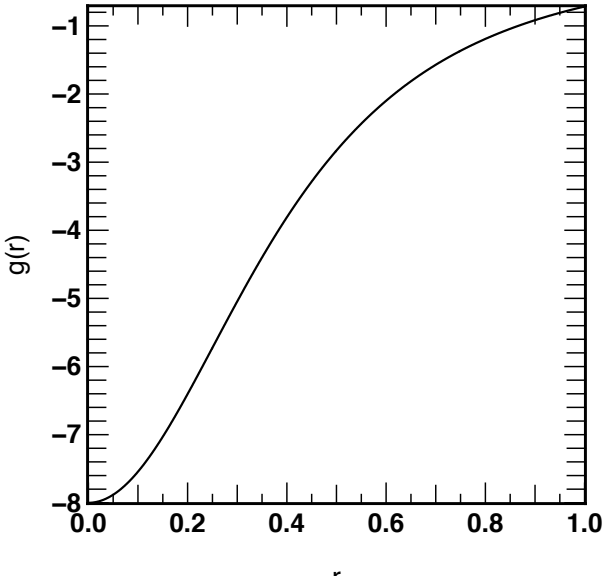

Cold case and softening: single oblique sine wave

Melott, Shandarin, Splinter & Suto 1997, ApJ 479, L79
Melott, 2007 arXiv 0709.0745

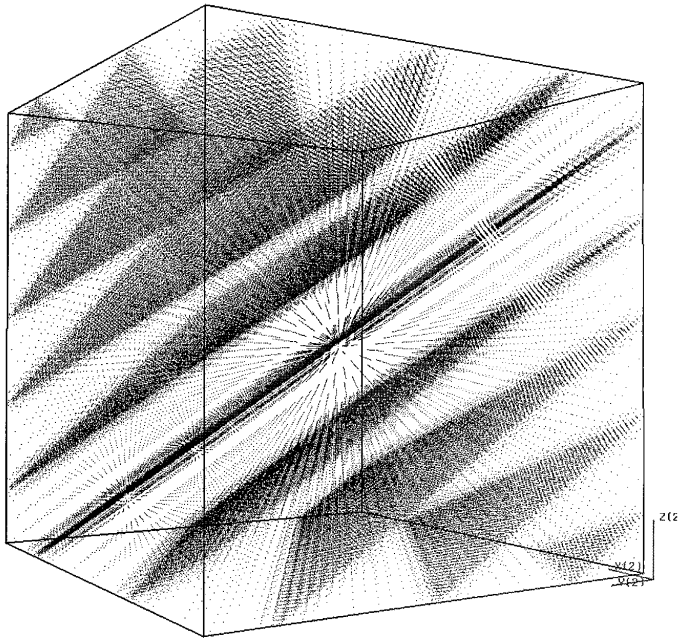

``Correct'' result at the end of the simulation

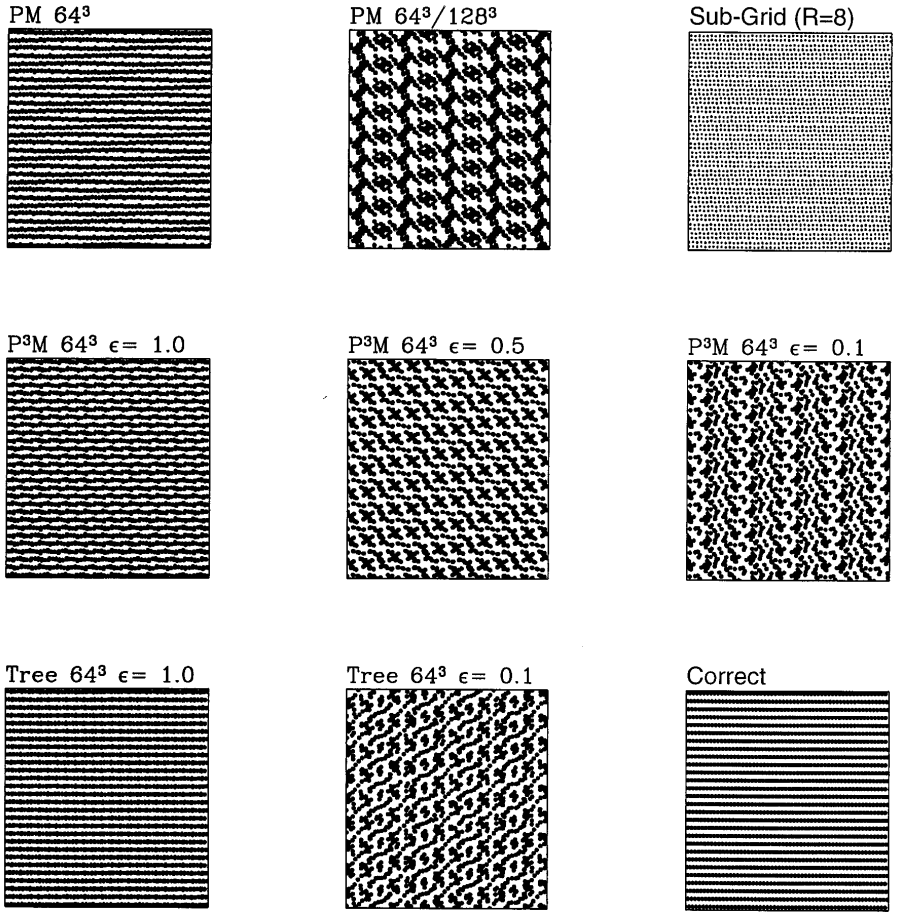

Various experiments

Direct Vlasov solvers

Two cases have to be considered: warm and cold

- Warm, when initial velocity dispersion is non negligible: relevant for galactic dynamics or for warm dark matter such as neutrinos
- Cold, when initial velocity dispersion is virtually null, such as in cold dark matter.

Warm case: numerous methods mainly invented for plasma physics, mostly of *semi-Lagrangian* nature (e.g. Yoshikawa, Yoshida & Umemura 2013, for a recent application in 6D phase-space). Among them:

- The *waterbag method*
- The *splitting algorithm* and its variants and improvements
- But many others: hydrodynamic upwind schemes, finite elements, etc

Bibliographic details: e.g. Alard & Colombi 2005, Sousbie & Scolombi 2016, Besse 2015: `http://www.vlasix.org/uploads/Main/Besse.pdf`

Cold case: the phase-space distribution is a D dimensional sheet moving in 2D dimensional phase-space. It is represented by an adaptive tessellation.

- Only 2 codes so far: Sousbie & Colombi 2016 (`ColDICE`) and Hahn & Angulo 2016

The cold case:
ColDICE: a parallel Vlasov-Poisson solver in 4D/6D using moving adaptive simplicial tessellation

Sousbie & Colombi, 2016, JCP 321, 644

See also Hahn & Angulo (2016) (as well as Shandarin et al., 2012, Abel et al., 2012, Hahn et al., 2015)

- In the cold case, solving Vlasov-Poisson equations can be reduced to following the evolution of a 3-dimensional sheet evolving in 6D phase-space (or a 2-dimensional one in 4D phase-space)

Initial conditions: $$f(\mathbf{r}, \mathbf{u}, t = t_\mathrm{i}) = \rho_\mathrm{i}(\mathbf{r})\, \delta_\mathrm{D}[\mathbf{u} - \mathbf{u}_\mathrm{i}(\mathbf{r})]$$

- The phase-space sheet is sampled with a self-adaptive conforming simplicial tessellation of which the vertices follow the equations of motion
- Poisson equation is solved on a grid of fixed resolution. The density on this grid is computed by computing the intersection of the projected tessellation with the grid with the method of Franklin Kankanhalli (1993, in Advances in spatial Databases, p. 477) generalized to linear order

Phase-space sheet tessellation: 2D

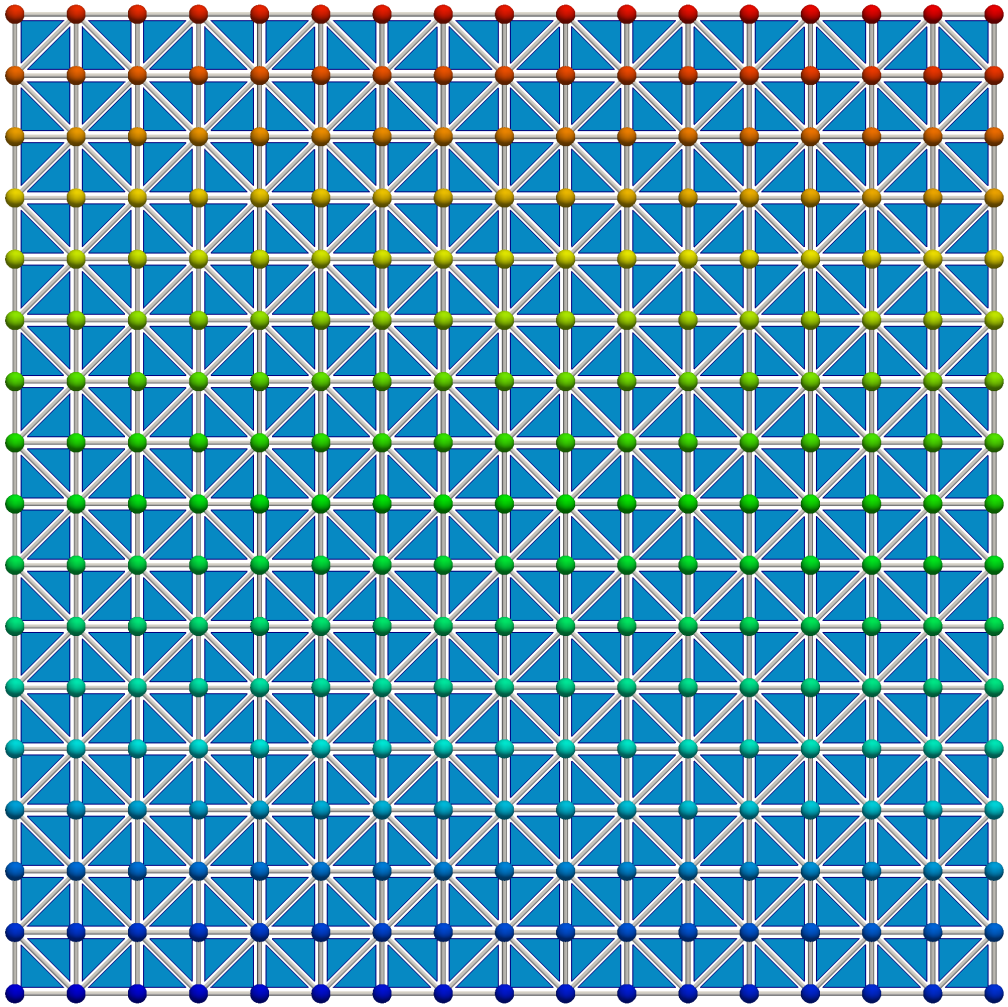

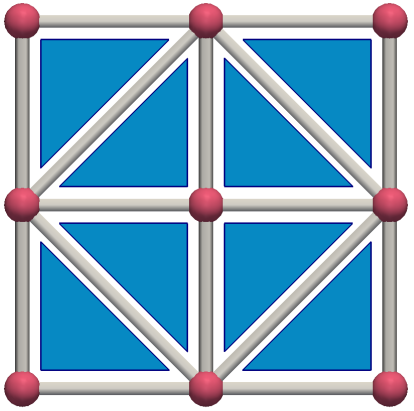

Abel, Hahn & Kaehler 2012; Shandarin, Habib & Heitmann 2012; Hahn, Abel & Kaehler 2013; Hahn & Angulo 2016; Sousbie & Colombi 2016

Phase-space sheet tessellation: 3D

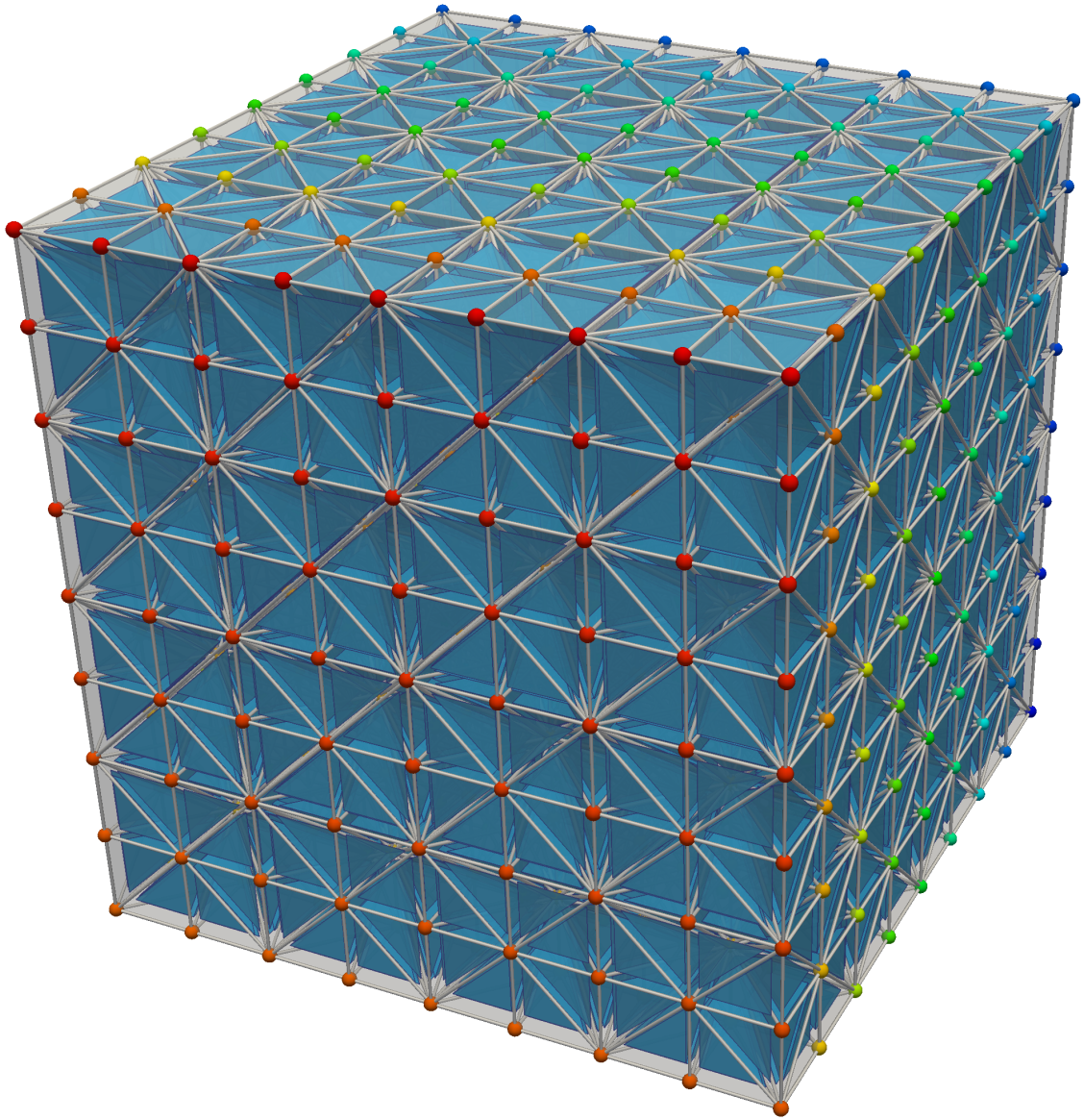

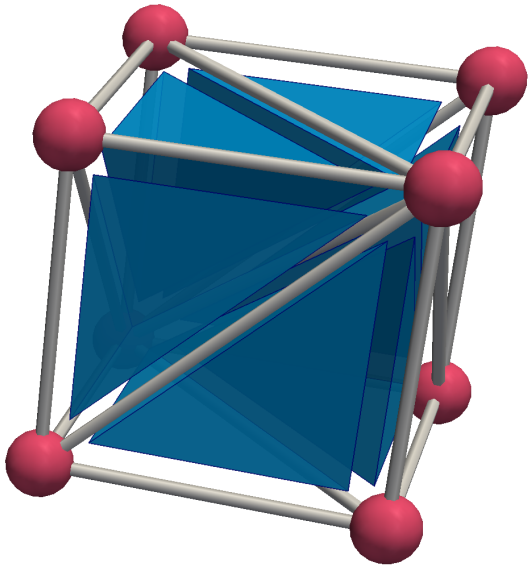

Resolution of Poisson equation: calculation of the projected density on a grid

Exact projected mass in a pixel/voxel

For V a pixel/voxel of a grid:

$$M(V) = \sum_i \int_{S_i \cap V} \rho_{\text{proj}}(\mathbf{x})\, d\mathbf{x}$$

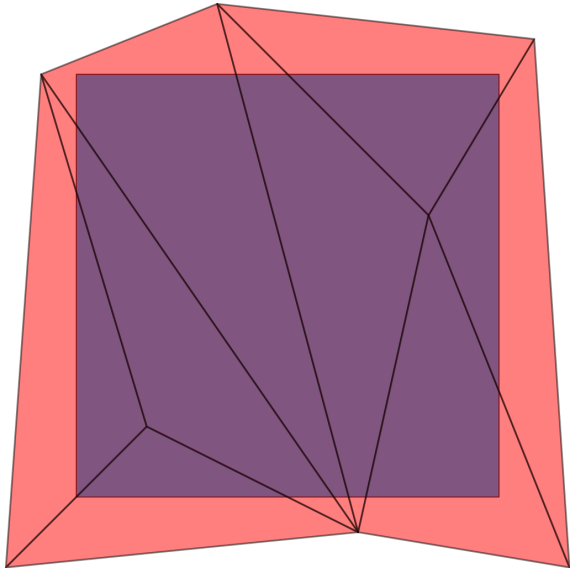

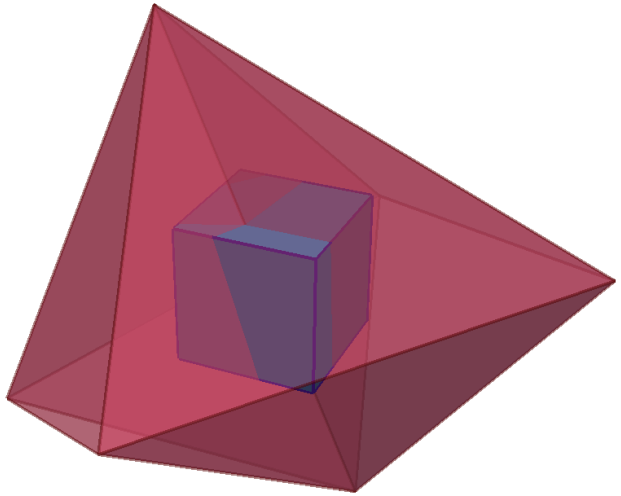

The Franklin & Kankanhalli method (Franklin 1983, 1987; Franklin & Kankanhalli, 1993)

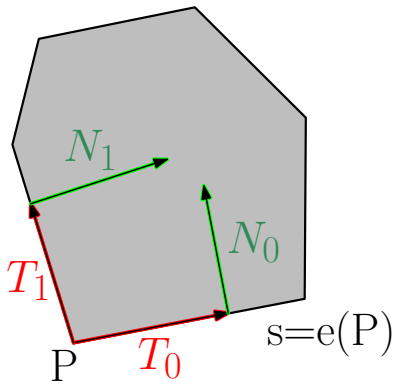

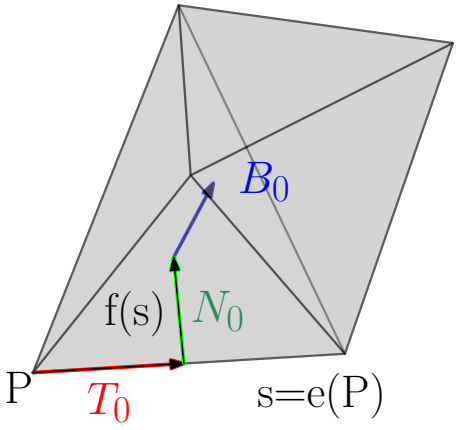

$$\mathrm{Vol}_{2D} = \frac{1}{2}\sum_{P}\sum_{e(P)} \mathbf{P.T}\,\mathbf{P.N}$$

$$\mathrm{Vol}_{3D} = -\frac{1}{6}\sum_{P}\sum_{s=e(P)}\sum_{f(s)} \mathbf{P.T}\,\mathbf{P.N}\,\mathbf{P.B}$$

$$M_0\left(V\right) = \sum \rho^0_{\mathrm{proj}}\,\mathrm{Vol}\left(V \cap S\right)$$

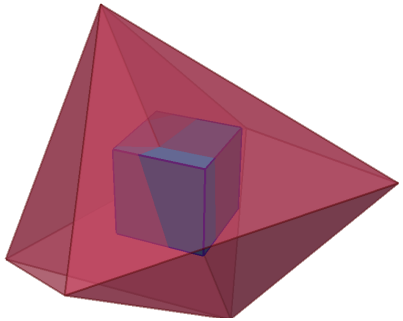

Generalization: Mass projection at order 1 (Sousbie & Colombi 2016)

$$M_1\left(V\right) = \sum_{(v,s_v,f_s)\in V} E_0\left(\rho^0_{\mathrm{proj}} + \mathbf{E_1}.\nabla\rho^1_{\mathrm{proj}}\right)$$

$$\text{with}\begin{cases} E_0^{3D} &= -\frac{1}{6}\mathbf{P.T}\,\mathbf{P.N}\,\mathbf{P.B}, \\ \mathbf{E_1^{3D}} &= \frac{1}{4}\left(\mathbf{P.T}\;\mathbf{T} + 2\mathbf{P.N}\;\mathbf{N} + 3\mathbf{P.B}\;\mathbf{B}\right). \end{cases}$$

Test particles versus tessellation projection in a 2D Plummer potential

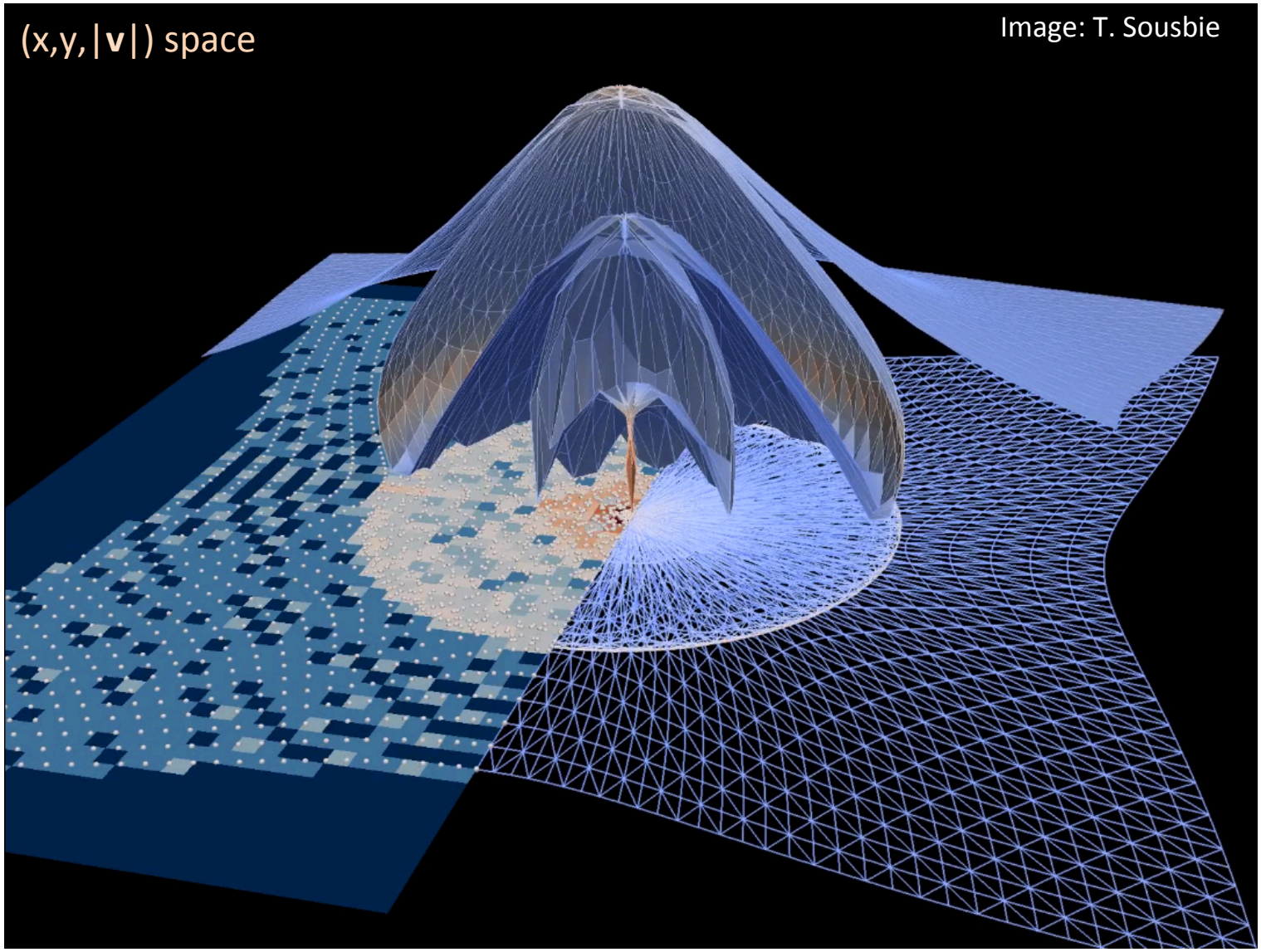

Refinement: based on measurements of Local Poincaré invariants

Poincaré invariant:
conserved along motion for an Hamiltonian system

$$I = \oint \mathbf{u}.\mathrm{d}\mathbf{r}(s)$$

Local Poincaré invariant
measured on a triangle
of the tessellation

$$\bar{I}_{jk} \equiv \frac{1}{2}\delta\mathbf{z_j}^{\mathsf{T}}\omega\,\delta\mathbf{z_k},$$

$$\omega = \begin{pmatrix} 0 & -\mathbf{I} \\ \mathbf{I} & 0 \end{pmatrix}.$$

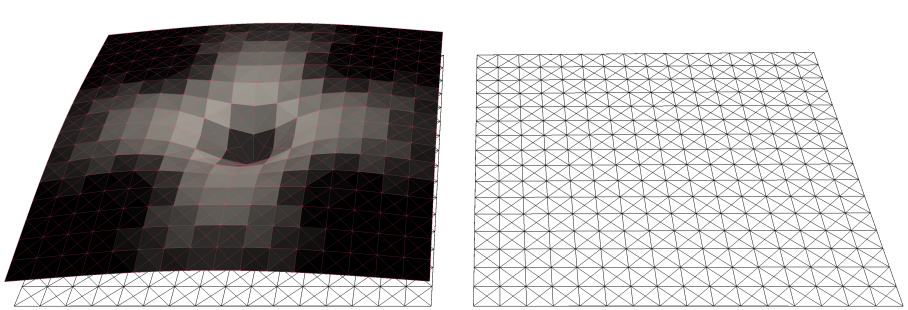

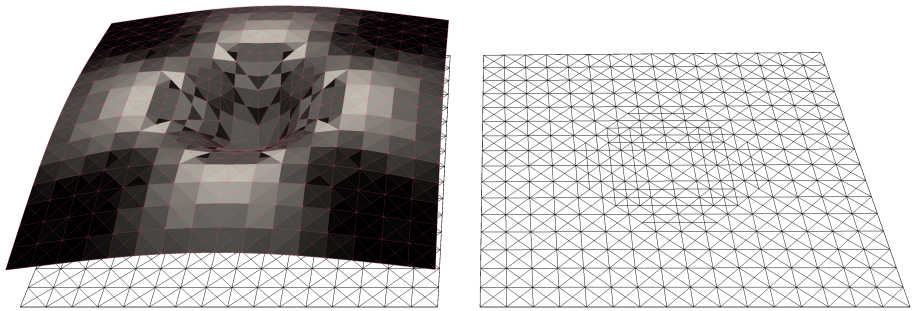

Refinement versus none in a 2D Plummer potential

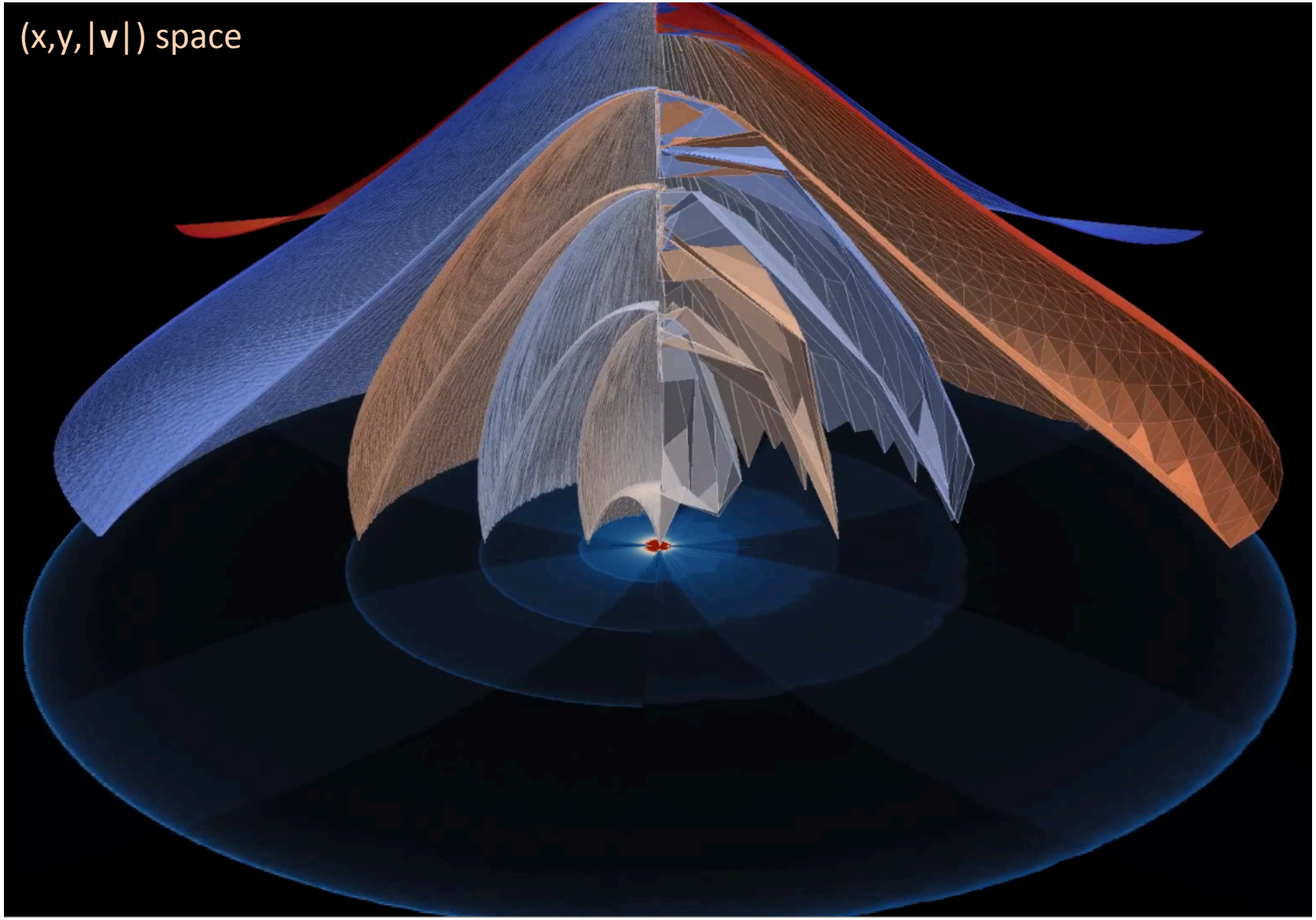

Image: T. Sousbie

Cosmological warm dark matter simulation in 3D (6D phase-space)
This is the way things would look for CDM at very small scales (solar system scale)
The first structure to form are pancakes

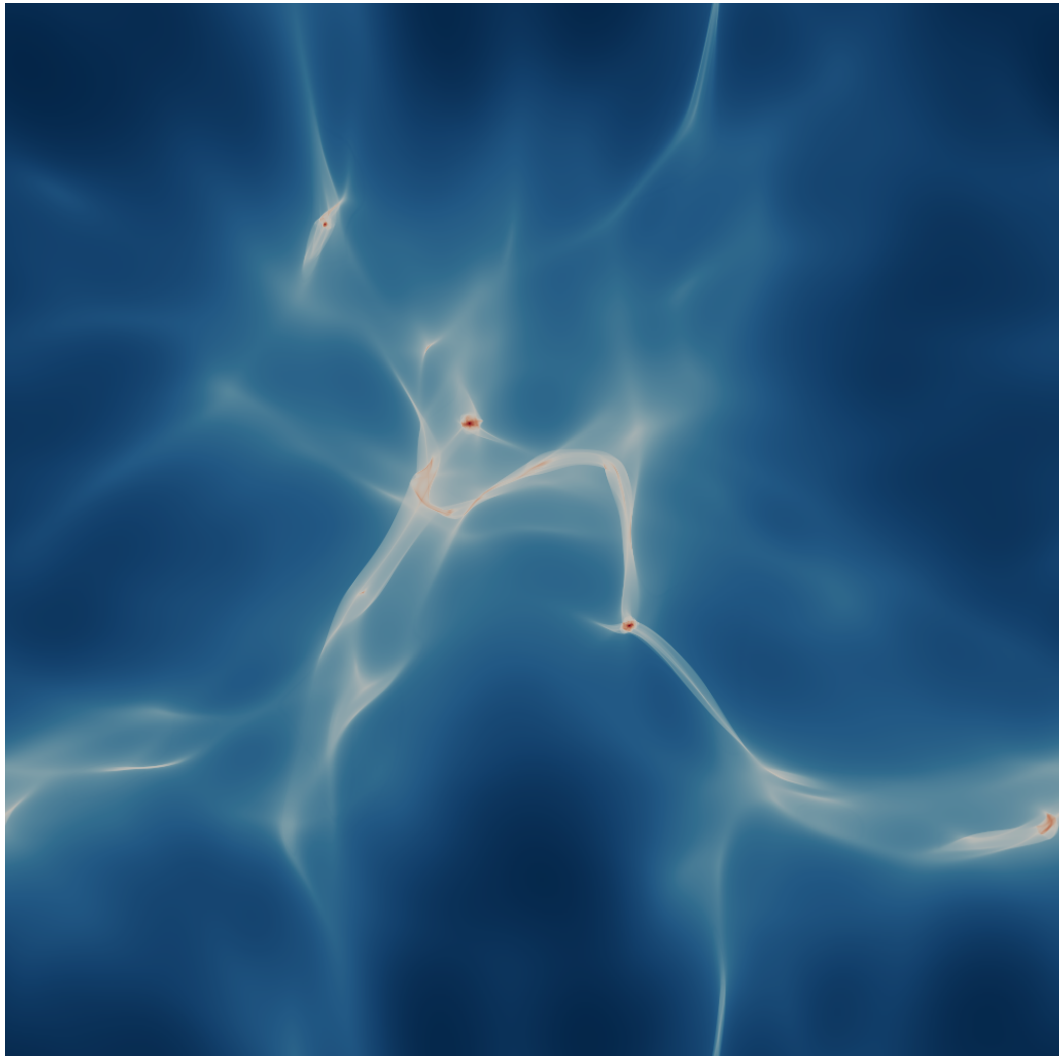

Projected density

Sousbie & Colombi 2016

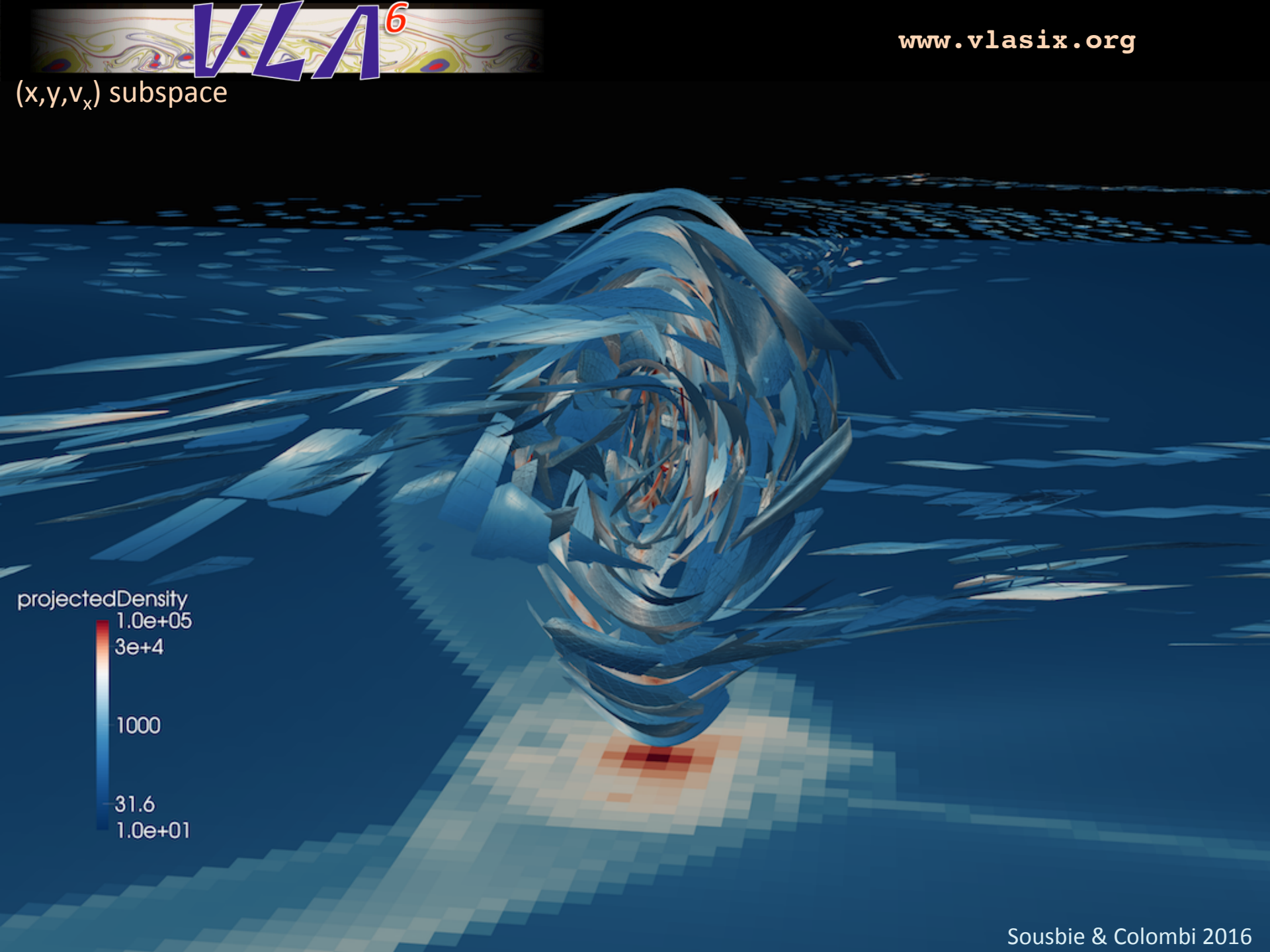
VLA 6
www.vlasix.org
(x,y,v_x) subspace
projectedDensity
1.0e+05
3e+4
1000
31.6
1.0e+01
Sousbie & Colombi 2016

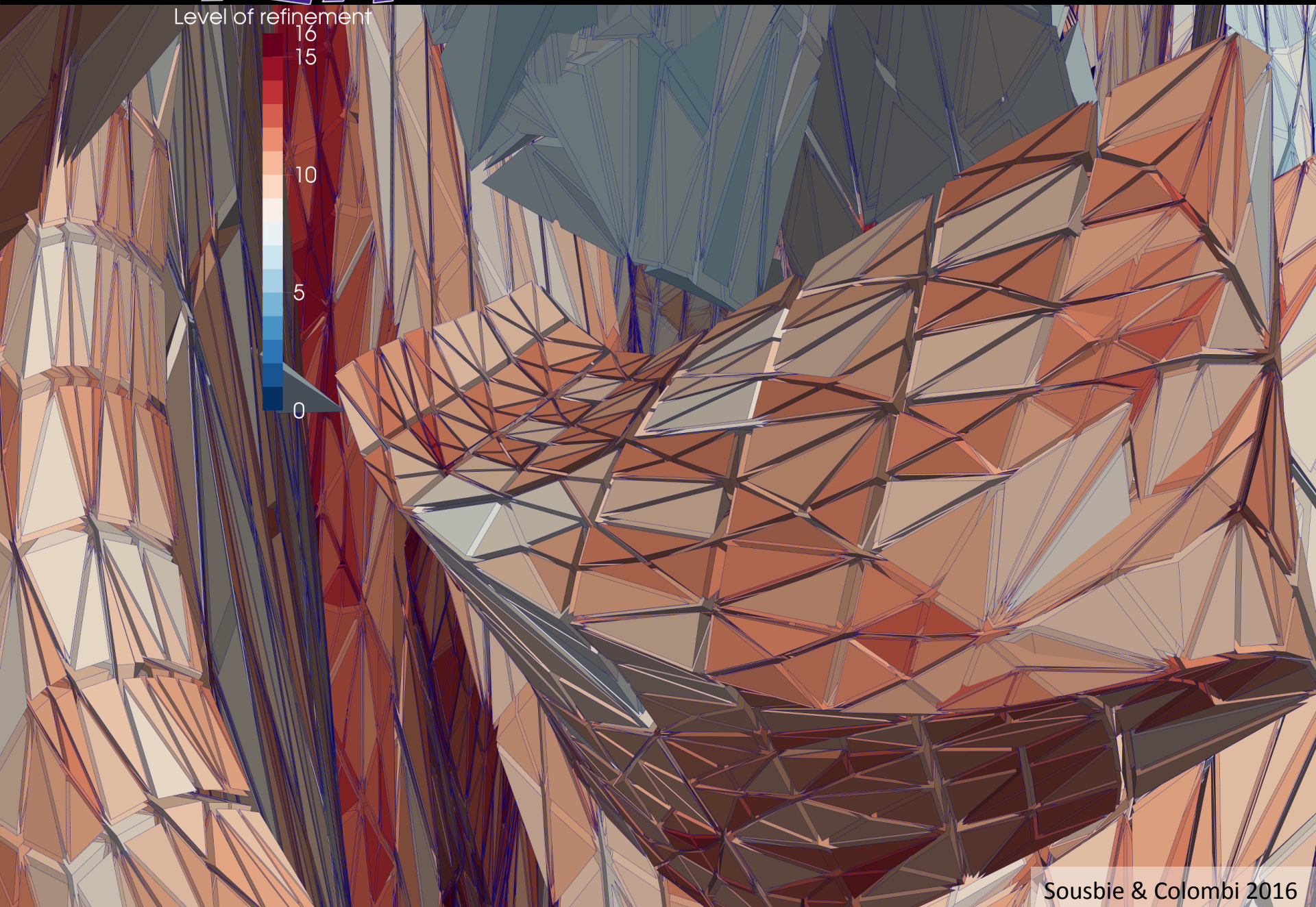

Sousbie & Colombi 2016

Dynamics of proto-halos

- **Highly simplified case:** 3 sine waves (Moutarde et al. 1991)
- **Lagrangian perturbation theory** (Zeldovich 1970, Bouchet et al. 1992, Buchert 1992)
- **High order Lagrangian perturbation theory** (Zheligovski & Frisch 2014, Rampf et al. 2015, Matsubara 2015, Saga, Taruya & Colombi 2018)
- **Quasi 1D Lagrangian perturbation theory** (Rampf & Frisch 2017)
- **Post-collapse perturbation theory** (Colombi 2014, Taruya & Colombi 2017)

2 sine waves with different amplitudes

Sousbie & Colombi 2016

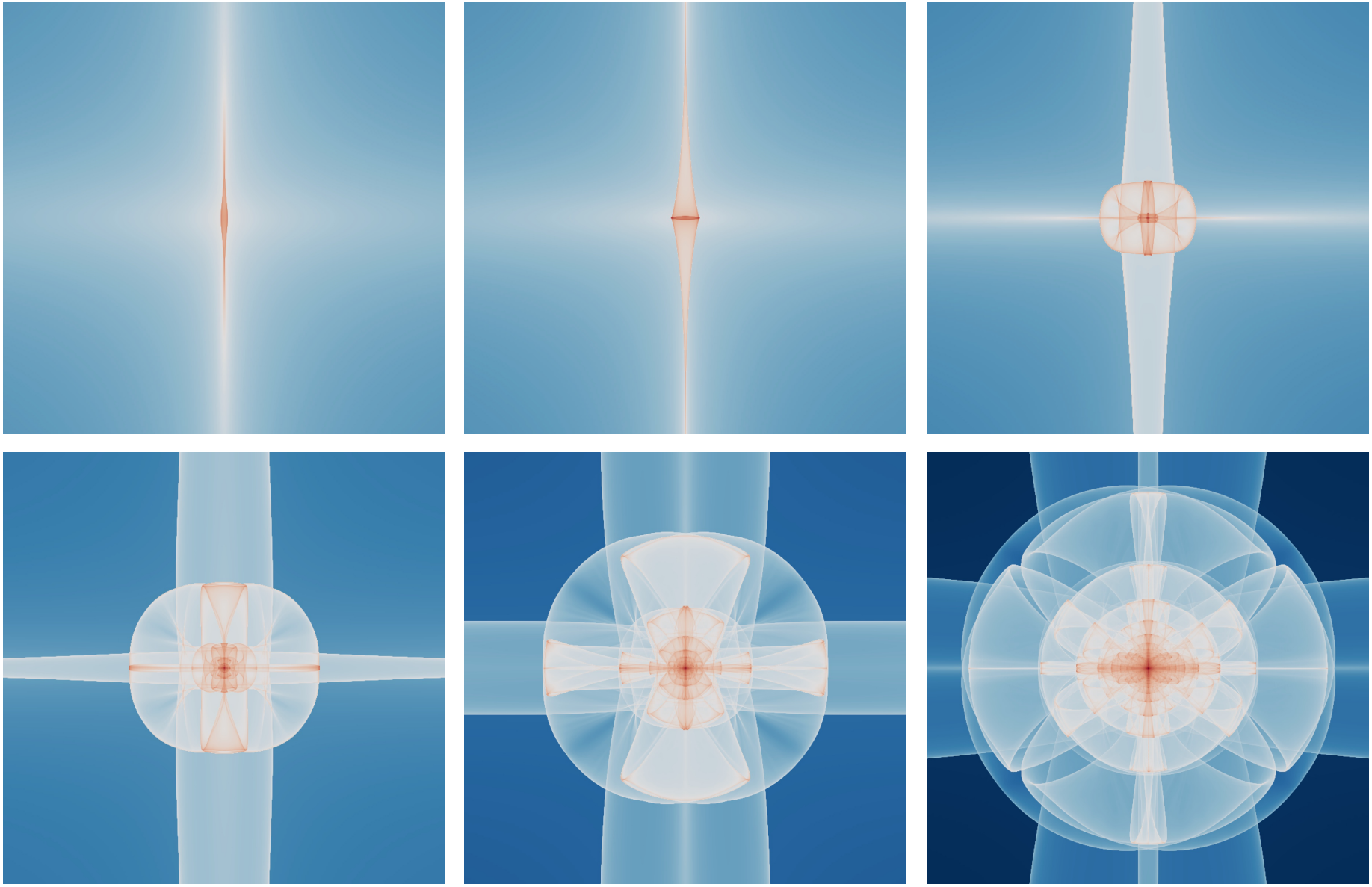

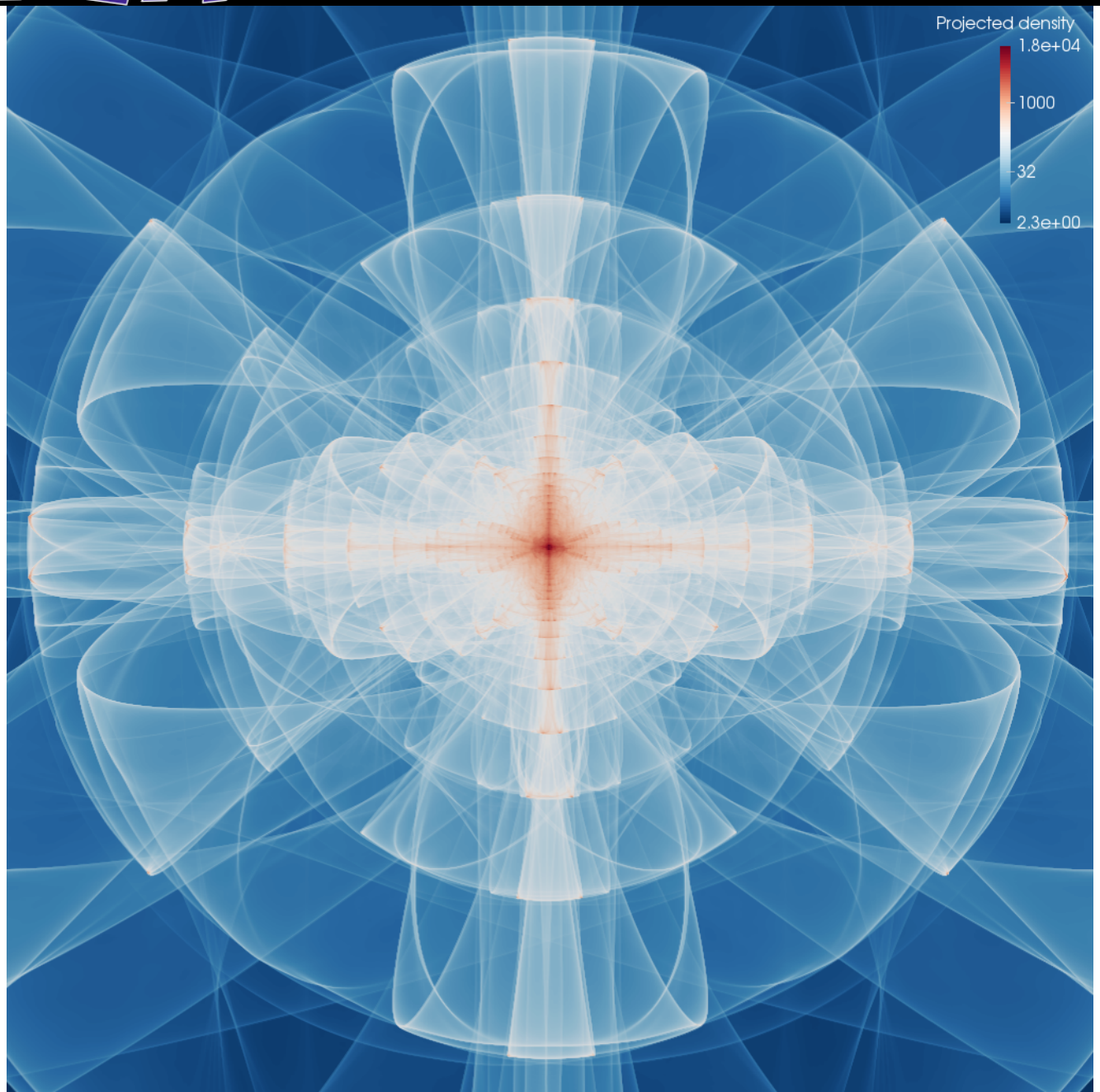

Sousbie & Colombi 2016

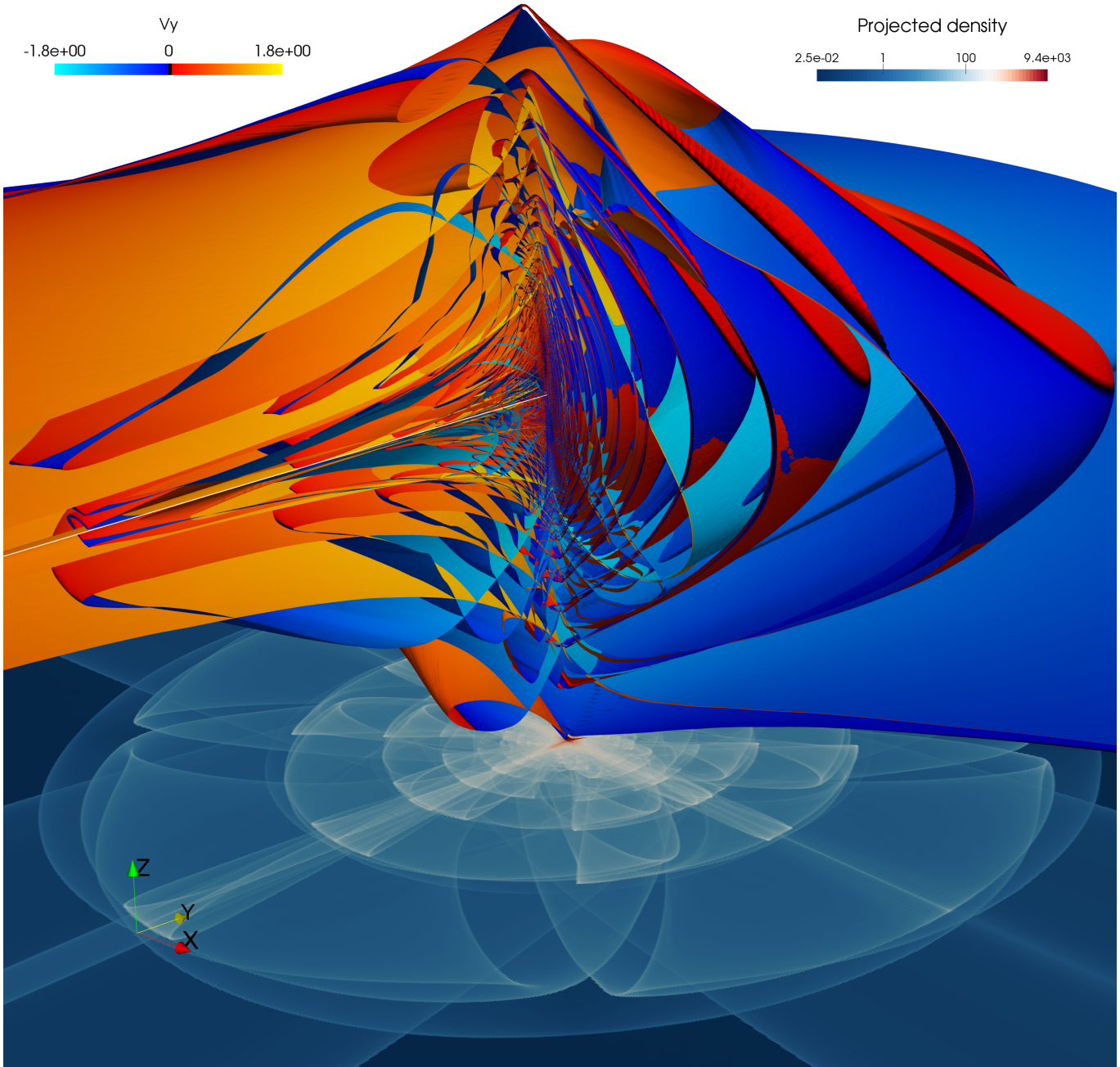

(x,y,v_x) space, color v_y

Sousbie & Colombi 2016

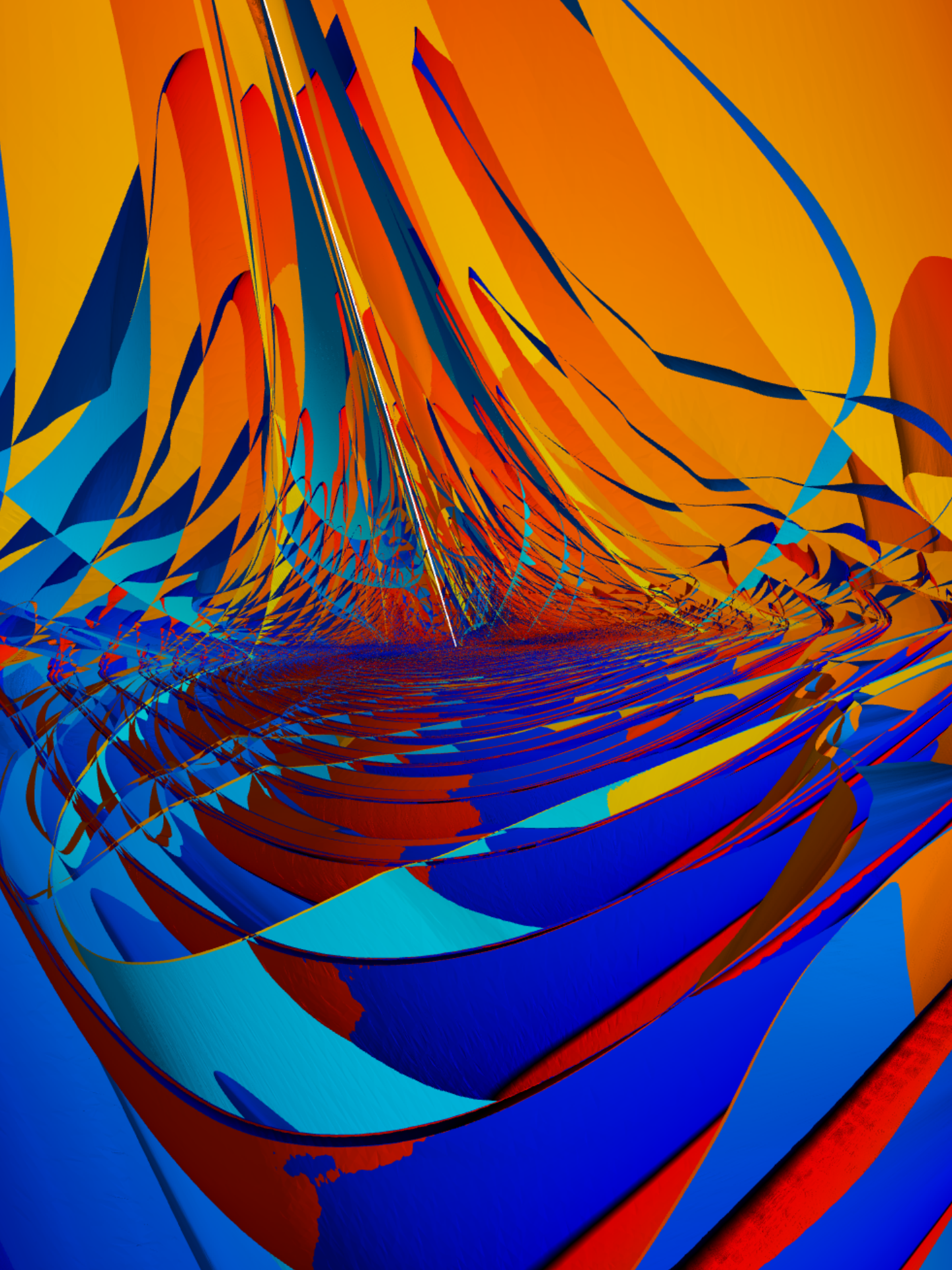

The 3D case: 3 sine waves with different amplitudes

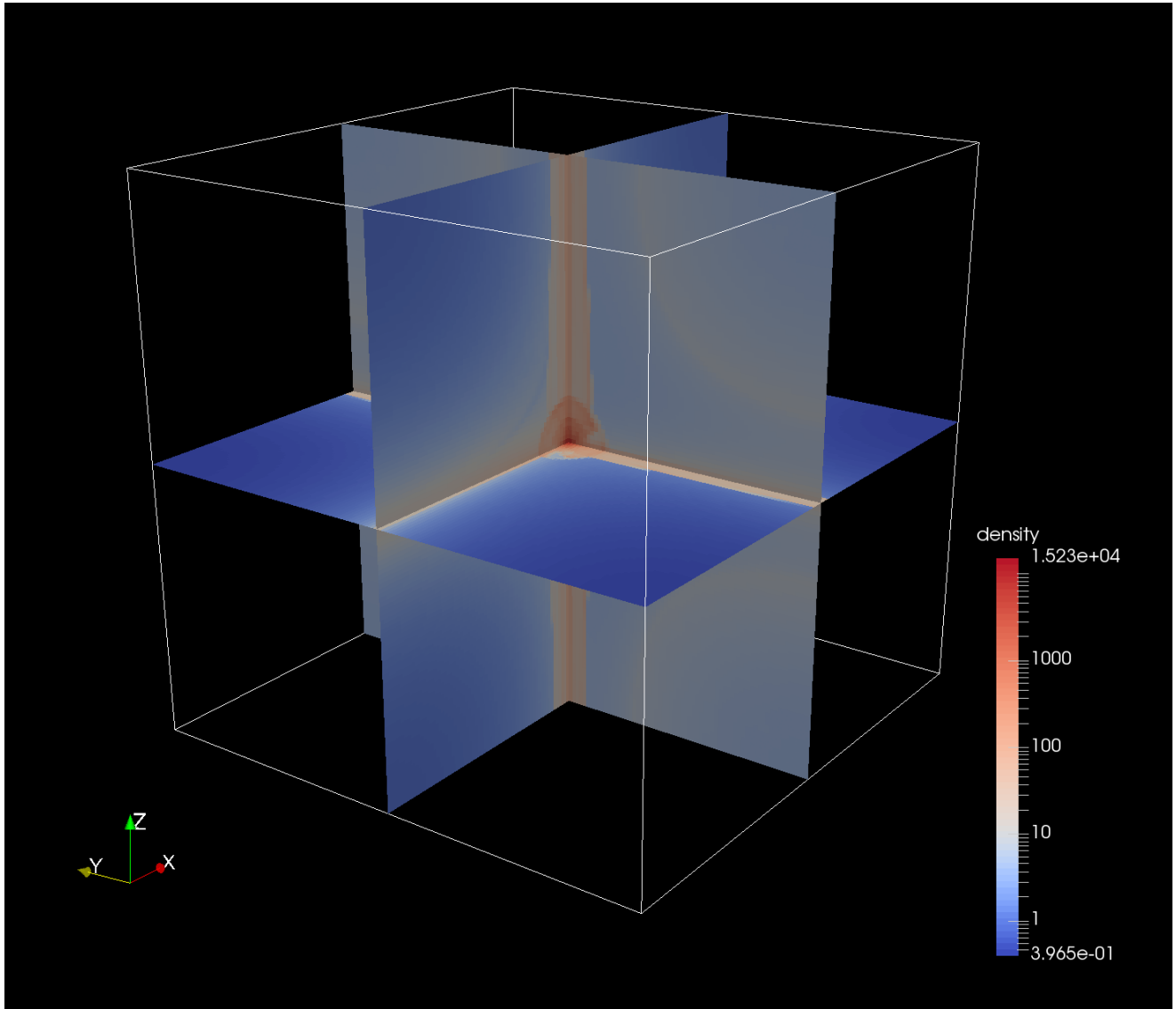

Colombi et al. 2018

The exquisite intersection of the phase-space sheet with the hyperplane x=y=0

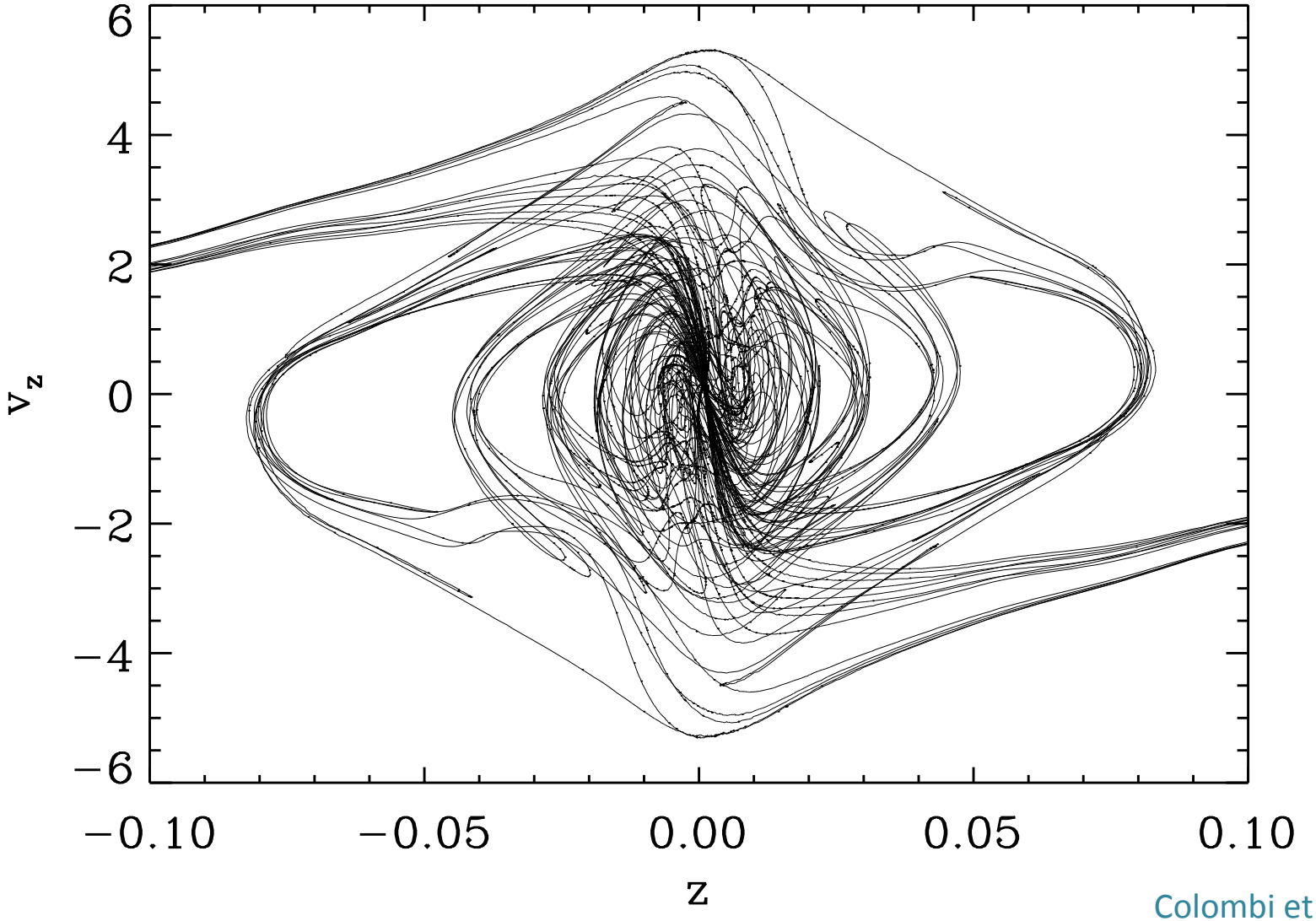

Colombi et al. 2018

Preliminary comparison with N-body (collaboration with S. Peirani)

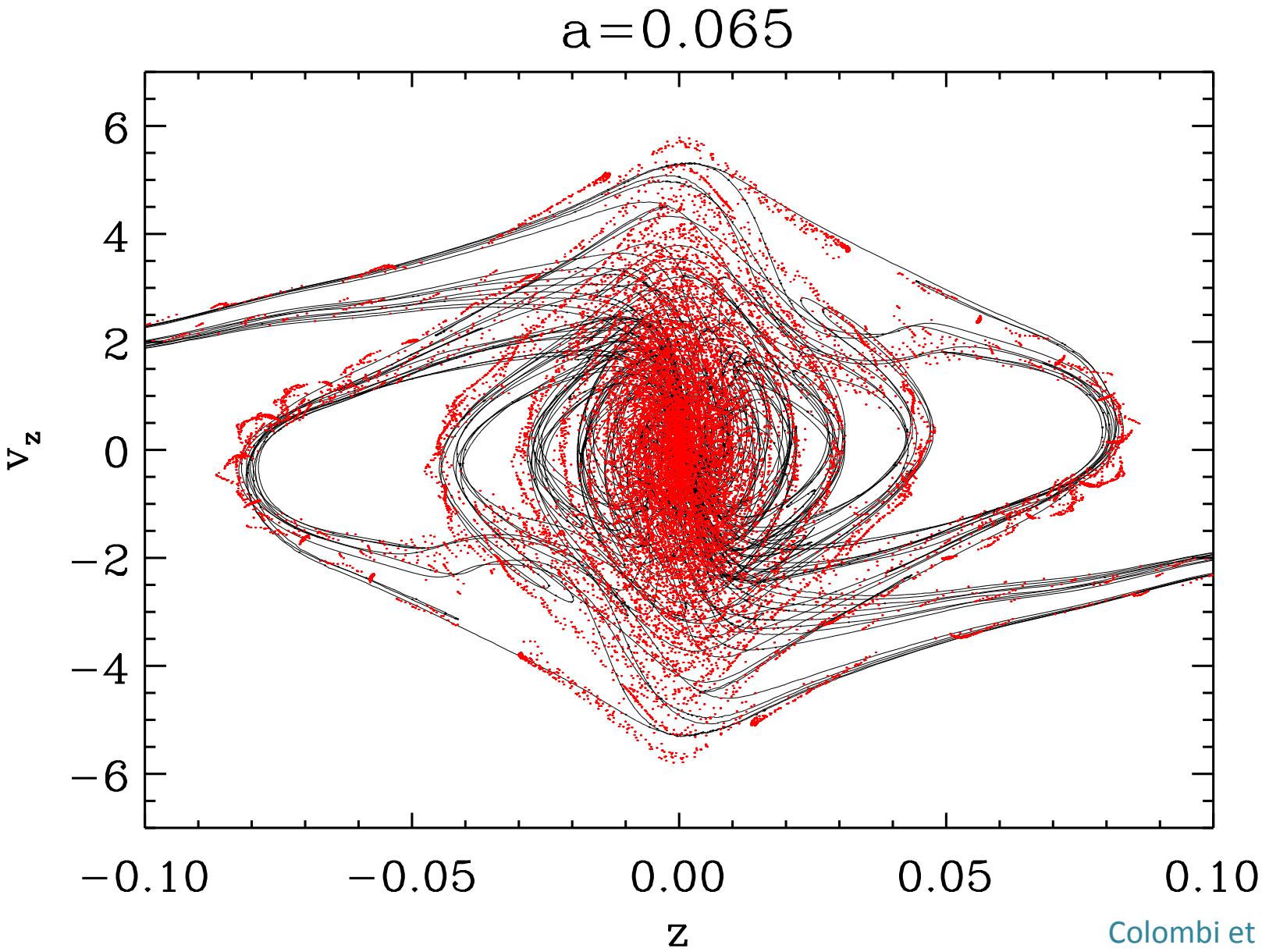

Colombi et al. 2018

Lagrangian equations of motion

See e.g., Matsubara 2015

Lagrangian equations of motion in the expanding Universe:

$$\ddot{\boldsymbol{x}} + 2H\dot{\boldsymbol{x}} = -\frac{1}{a^2}\boldsymbol{\nabla}_x\phi(\boldsymbol{x}) \ ,$$
$$\boldsymbol{\nabla}_x^2\phi(\boldsymbol{x}) = 4\pi G\bar{\rho}_{\rm m}a^2\delta(\boldsymbol{x})$$

a : scale factor of the Universe
$\rho_{\rm m}$: average matter density
δ : density contrast

Lagrangian displacement field: $\boldsymbol{\Psi}(t,\boldsymbol{q})$

$$\boldsymbol{x}(t,\boldsymbol{q}) \ = \ \boldsymbol{q} + \boldsymbol{\Psi}(t,\boldsymbol{q})$$
$$\boldsymbol{v}(t,\boldsymbol{q}) \ = \ a(t)\dot{\boldsymbol{\Psi}}(t,\boldsymbol{q})$$

Divergence: longitudinal part: $\boldsymbol{\nabla}_x \cdot \left[\ddot{\boldsymbol{\Psi}}(t,\boldsymbol{q}) + 2H\dot{\boldsymbol{\Psi}}(t,\boldsymbol{q})\right] = -4\pi G\bar{\rho}_{\rm m}\delta(\boldsymbol{x})$

Curl: transverse part: $\boldsymbol{\nabla}_x \times \left[\ddot{\boldsymbol{\Psi}}(t,\boldsymbol{q}) + 2H\dot{\boldsymbol{\Psi}}(t,\boldsymbol{q})\right] = 0 \ ,$

Mass conservation: $1 + \delta(\boldsymbol{x}) = 1/\det\left(\delta_{ij} + \Psi_{i,j}\right)$

Lagrangian perturbation theory

See e.g., Matsubara 2015

Perturbative expansion: $$\boldsymbol{\Psi}(\tau, \boldsymbol{q}) = \sum_{n=1}^{\infty} \boldsymbol{\Psi}^{(n)}(\tau, \boldsymbol{q})$$

$$\tau \equiv \ln D_+ = \ln a$$

Einstein de Sitter : $\Omega_{\mathrm{m},0} = 1$

Longitudinal:

$$\left(\hat{\mathcal{T}} - \frac{3}{2}\right) \Psi^{(n)}_{k,k} = -\epsilon_{ijk}\epsilon_{ipq} \sum_{n=m_1+m_2} \Psi^{(m_1)}_{j,p} \left(\hat{\mathcal{T}} - \frac{3}{4}\right) \Psi^{(m_2)}_{k,q}$$

$$-\frac{1}{2}\epsilon_{ijk}\epsilon_{pqr} \sum_{n=m_1+m_2+m_3} \Psi^{(m_1)}_{i,p} \Psi^{(m_2)}_{j,q} \left(\hat{\mathcal{T}} - \frac{1}{2}\right) \Psi^{(m_3)}_{k,r} \ ,$$

Transverse:

$$\epsilon_{ijk}\hat{\mathcal{T}}\Psi^{(n)}_{j,k} = -\epsilon_{ijk} \sum_{n=m_1+m_2} \Psi^{(m_1)}_{p,j} \hat{\mathcal{T}} \Psi^{(m_2)}_{p,k}$$

Time operator: $$\hat{\mathcal{T}} \equiv \frac{\partial^2}{\partial \tau^2} + \frac{1}{2}\frac{\partial}{\partial \tau}$$

Solution reconstruction: $$\boldsymbol{\Psi}^{(n)} = \triangle^{-1}\left[\boldsymbol{\nabla}\left(\boldsymbol{\nabla}\cdot\boldsymbol{\Psi}^{(n)}\right) - \boldsymbol{\nabla}\times(\boldsymbol{\nabla}\times\boldsymbol{\Psi})\right]$$

Setup and various PT approximations

Saga, Taruya & Colombi 2018, arXiv:1805.08787

- **3 sine waves** in a periodic box: $\Psi^{\rm ini}(\boldsymbol{q}) = \frac{L}{2\pi}\begin{pmatrix} \epsilon_x \sin\left(\frac{2\pi}{L}q_x\right) \\ \epsilon_y \sin\left(\frac{2\pi}{L}q_y\right) \\ \epsilon_z \sin\left(\frac{2\pi}{L}q_z\right) \end{pmatrix}$

(ϵ_x, ϵ_y, ϵ_z)=(-24, -4, -3) : ''quasi'' 1D
(-24, -18, -12) : "normal"
(-18, -18, -18) : ''Isotropic''

$a_{\rm ini}$=0.0005

- **Quasi 1D :** $|\epsilon_x| >> |\epsilon_y|, |\epsilon_z|$

$$\Psi^{(0)}(\tau,\boldsymbol{q}) = e^{\tau}(\Psi_x^{\rm ini}(q_x),0,0)$$
$$\Psi^{(1)}(\tau,\boldsymbol{q}) = e^{\tau}(0,\Psi_y^{\rm ini}(q_y),\Psi_z^{\rm ini}(q_z))$$

1st and 2nd order

- **Full PT with all the terms** (including decaying modes): up to 5th order
- **PT with only fastest growing modes:** up to 10th order
- **Extrapolation to infinite order** using results up to 10th order PT

$$A_{\rm sc}(\boldsymbol{q},n) = \alpha_A(\boldsymbol{q}) + \frac{1}{b_A(\boldsymbol{q}) + c_A(\boldsymbol{q})\exp\left[d_A(\boldsymbol{q})\, n^{e_A(\boldsymbol{q})}\right]}$$

Trying to capture the structure at collapse in 3D: high order perturbation theory

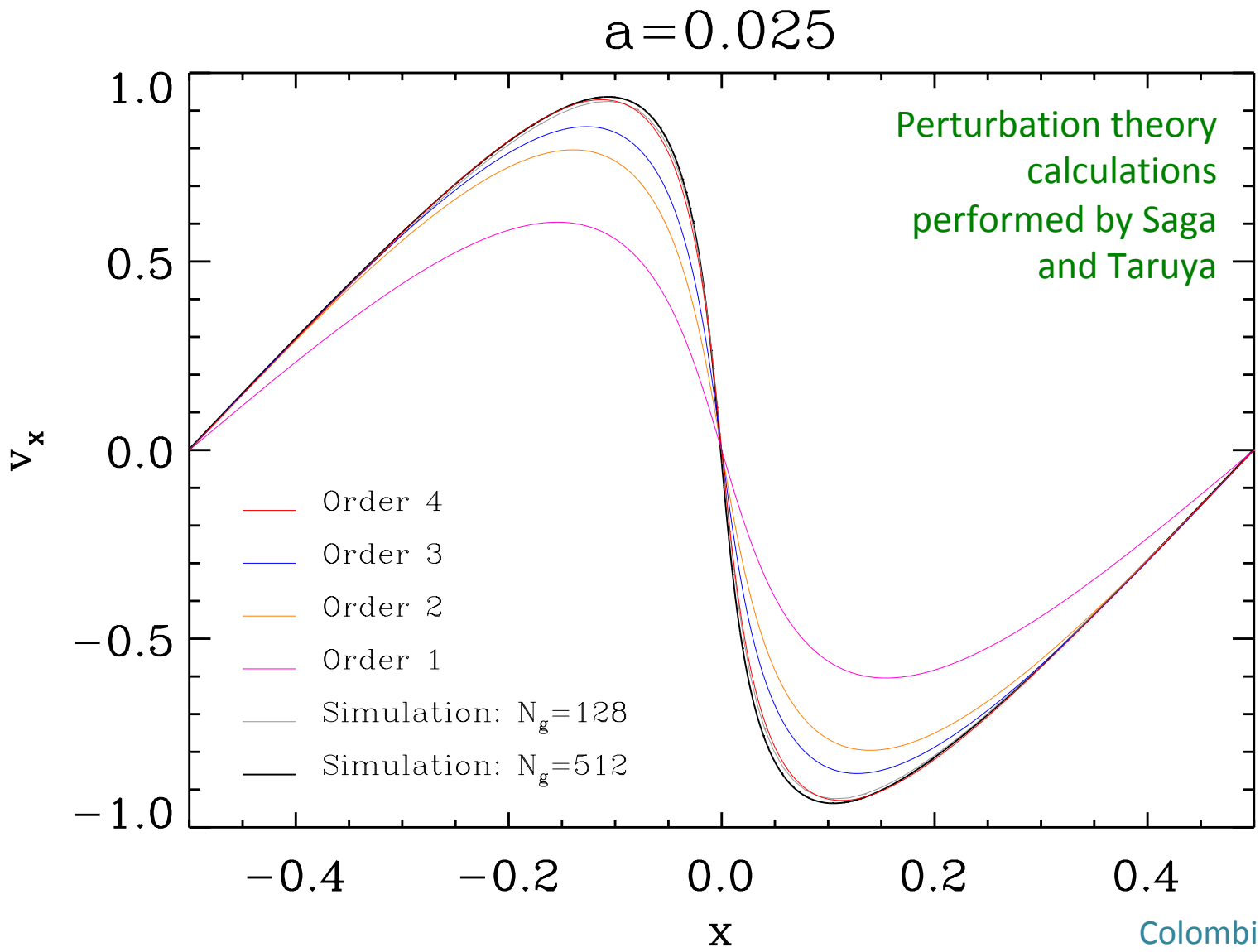

Colombi et al. 2018

At collapse time: convergence of the perturbative series seems very slow

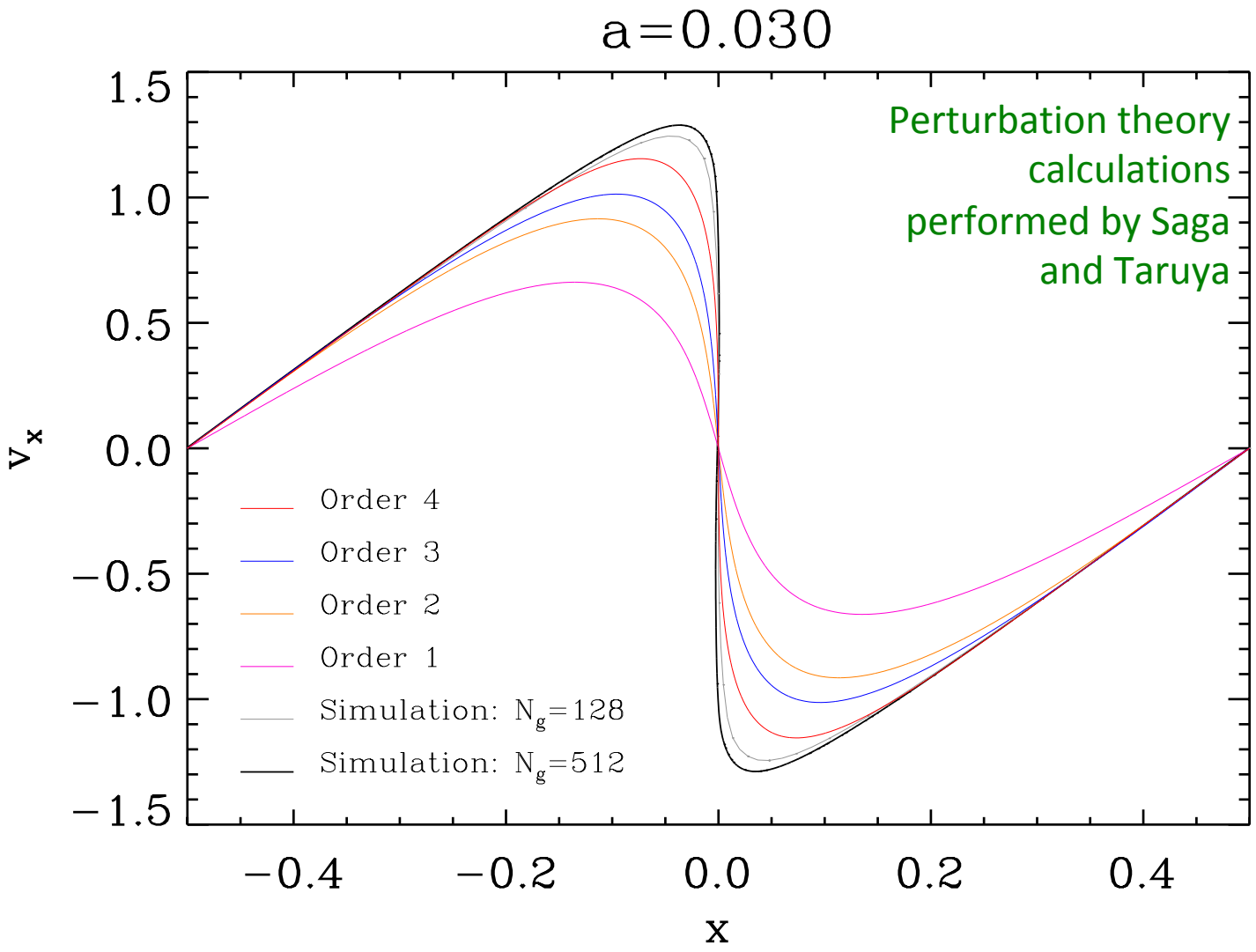

Colombi et al. 2018

The post collapse regime…

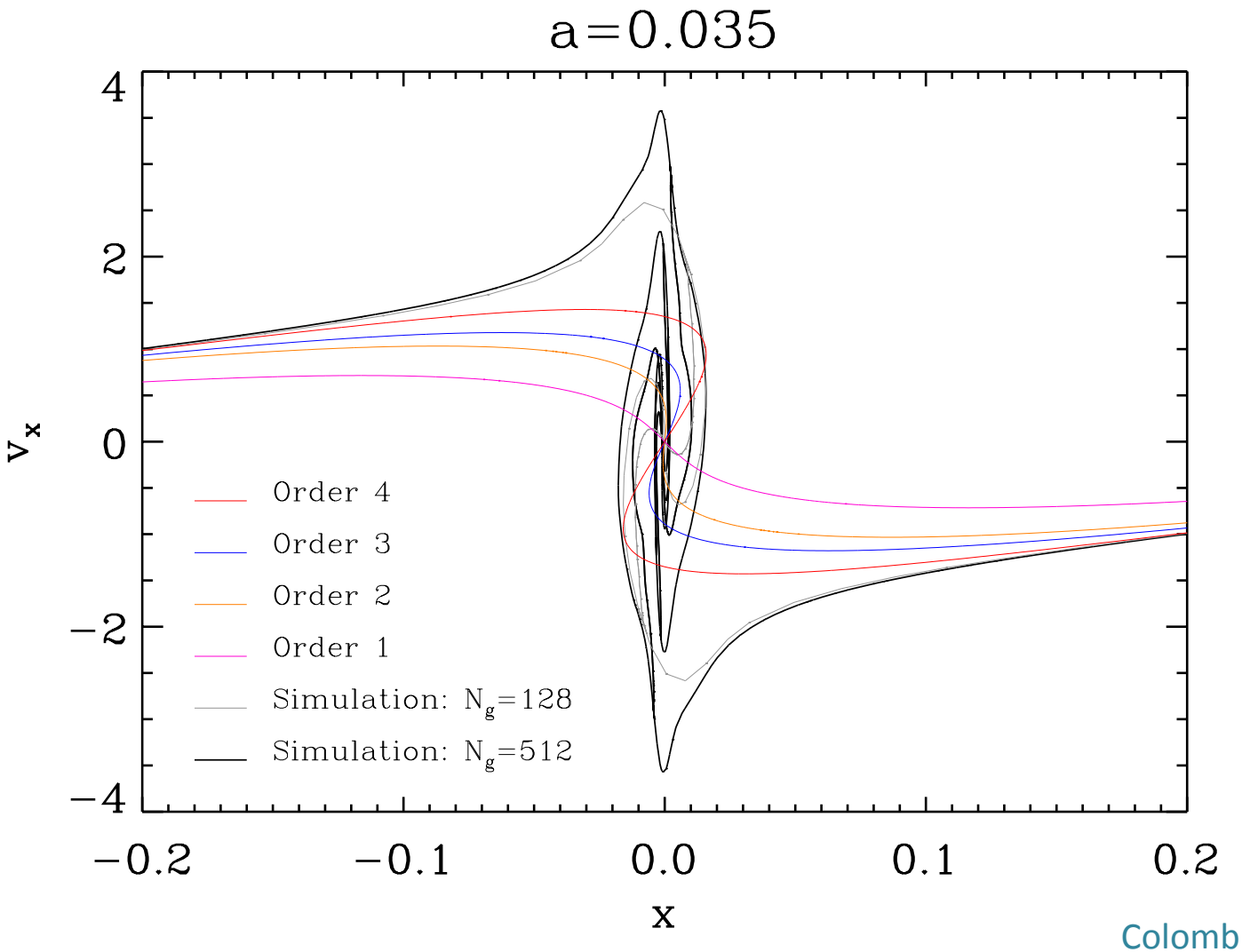

Colombi et al. 2018

After several dynamical times…

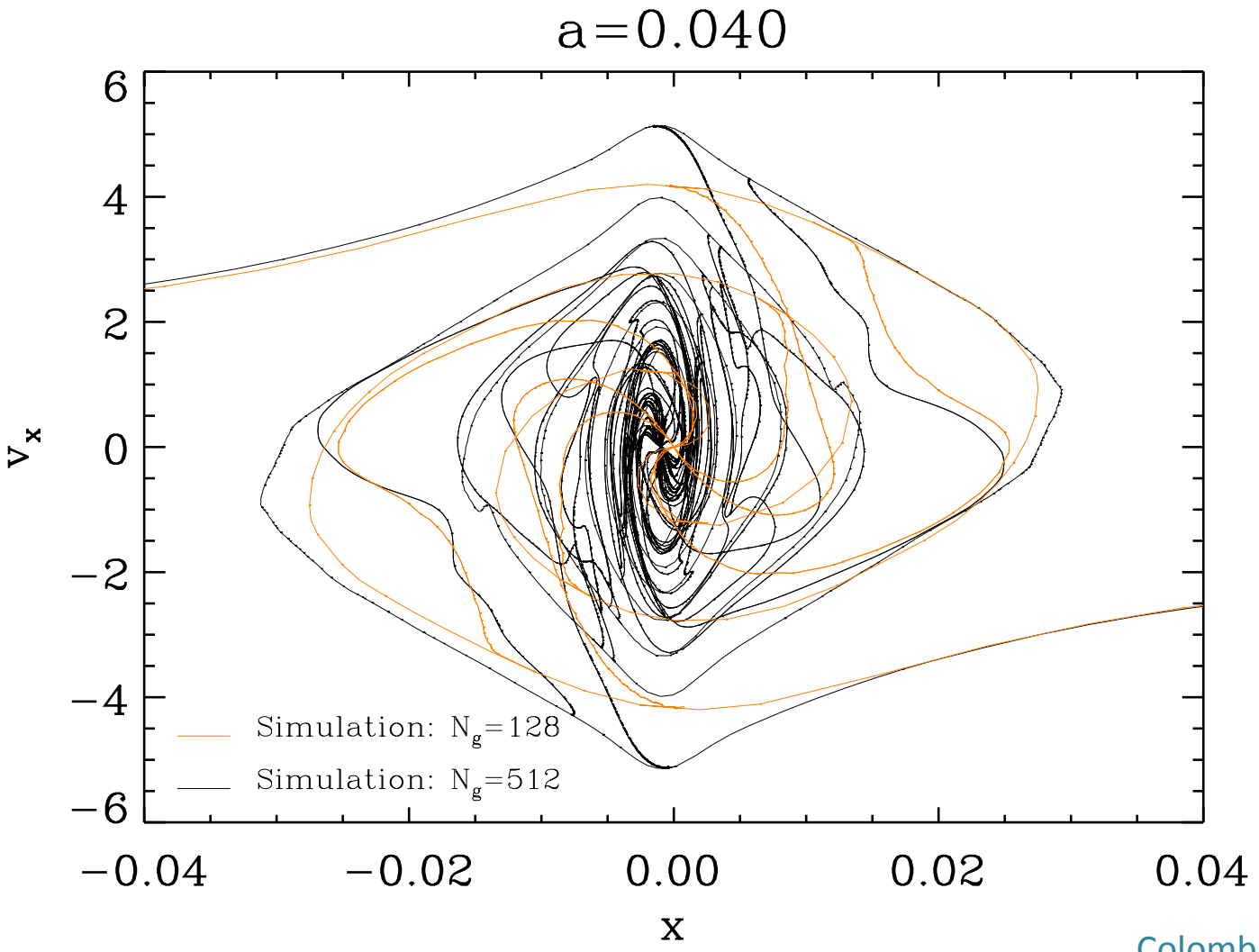

Colombi et al. 2018

Quasi 1D case

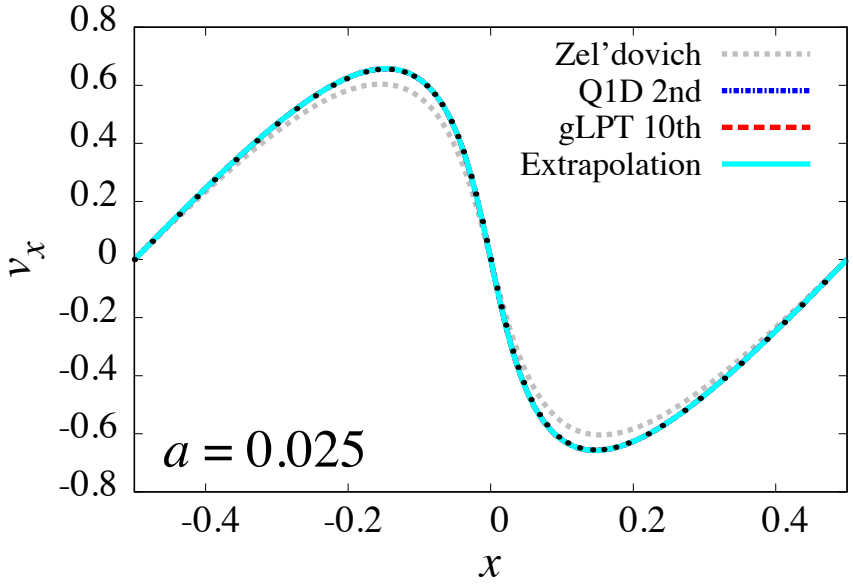

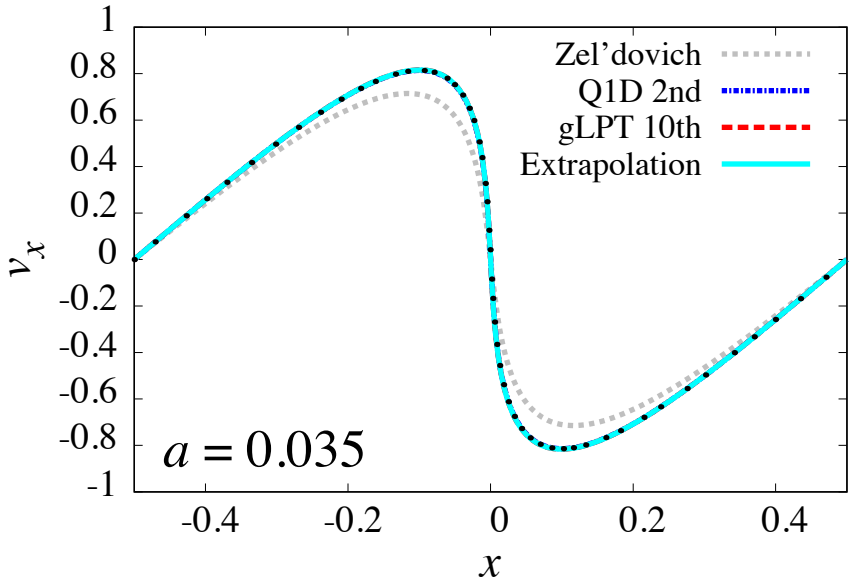

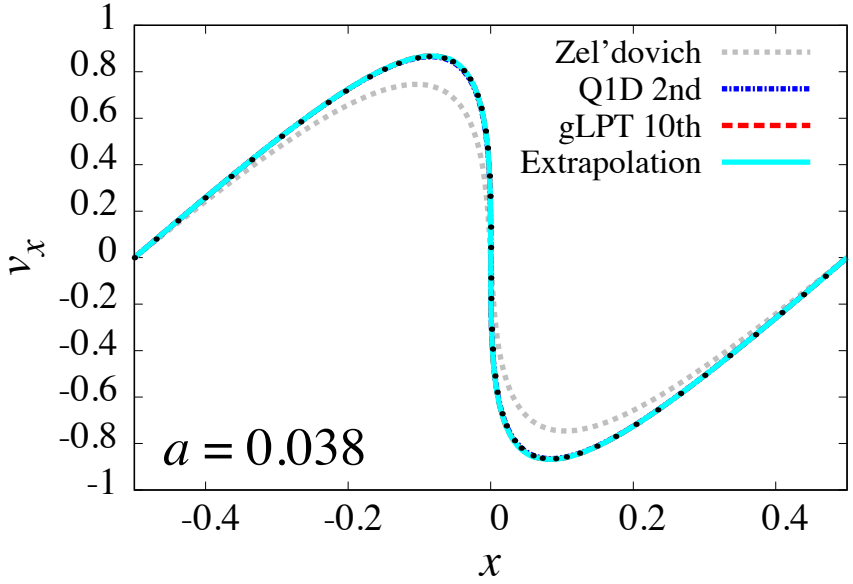

$(\varepsilon_x, \varepsilon_y, \varepsilon_z)=(-24,\ -4,\ -3)$

Saga, Taruya & Colombi 2018
arXiv:1805.08787

"Typical" case

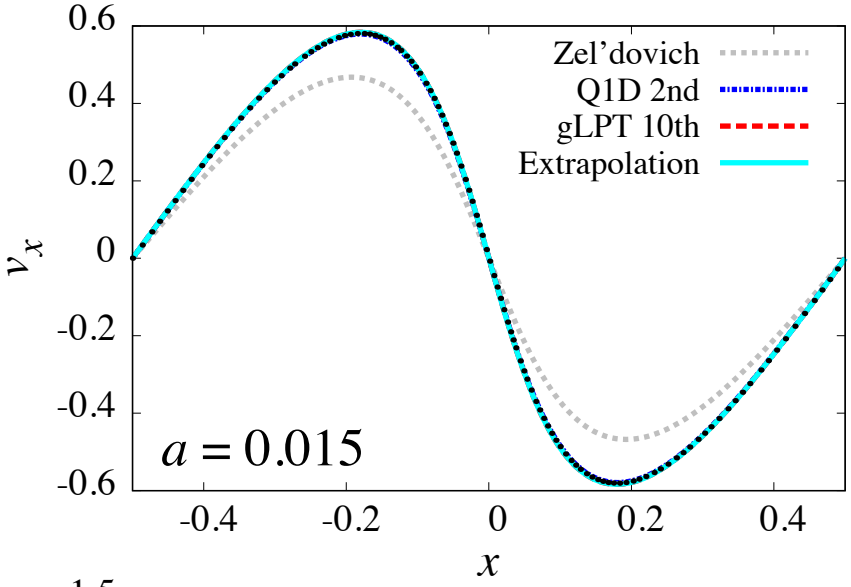

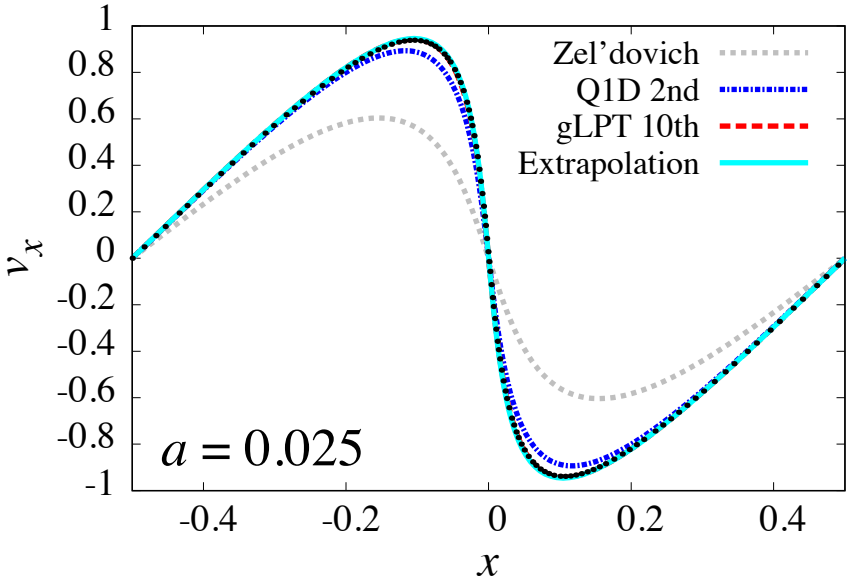

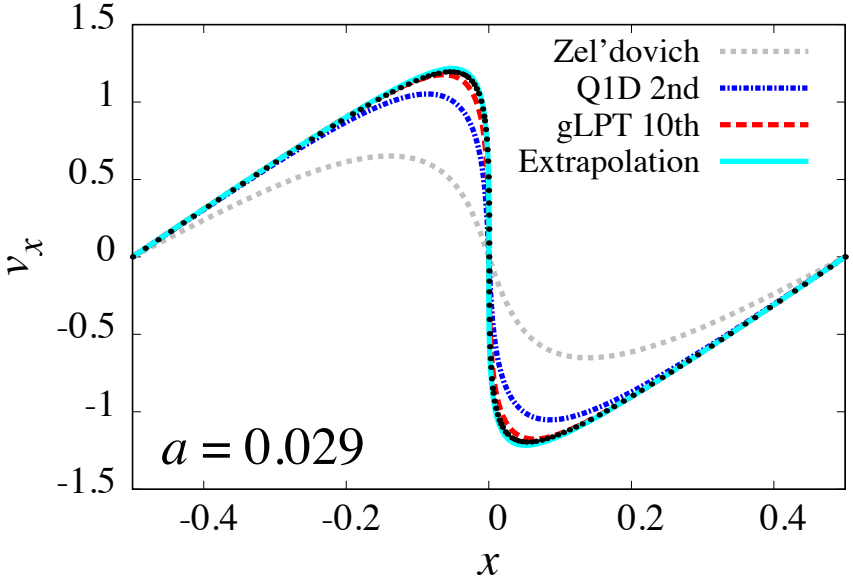

$(\varepsilon_x, \varepsilon_y, \varepsilon_z)=(-24, -18, -12)$

Saga, Taruya & Colombi 2018
arXiv:1805.08787

"Isotropic" case

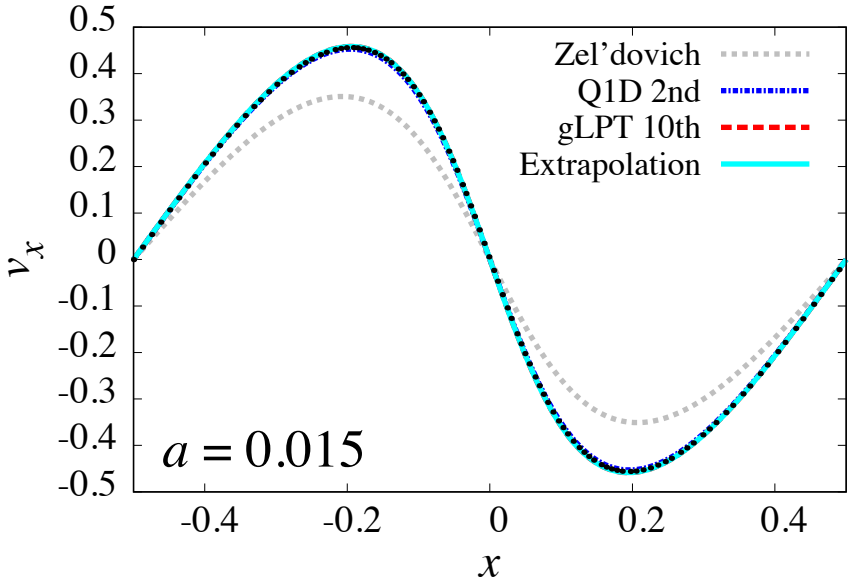

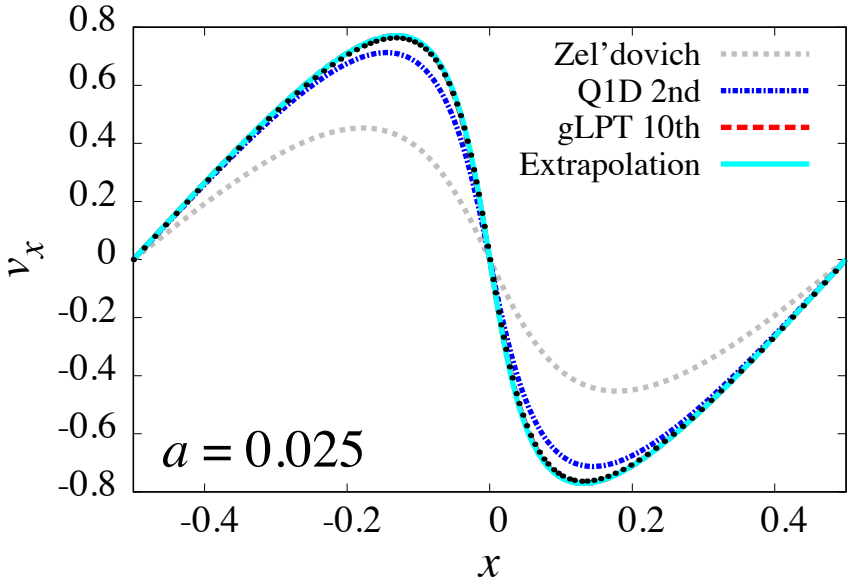

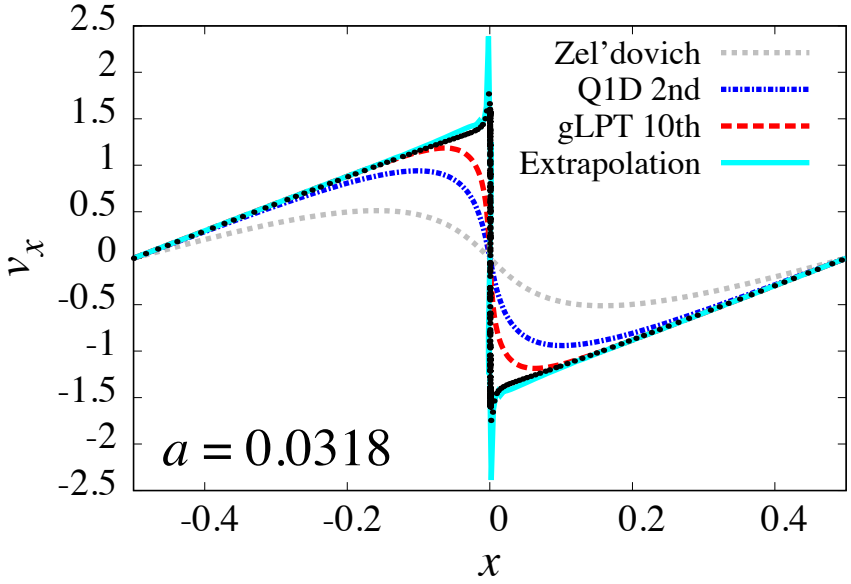

$(\varepsilon_x, \varepsilon_y, \varepsilon_z)=(-18, -18, -18)$

Saga, Taruya & Colombi 2018
arXiv:1805.08787

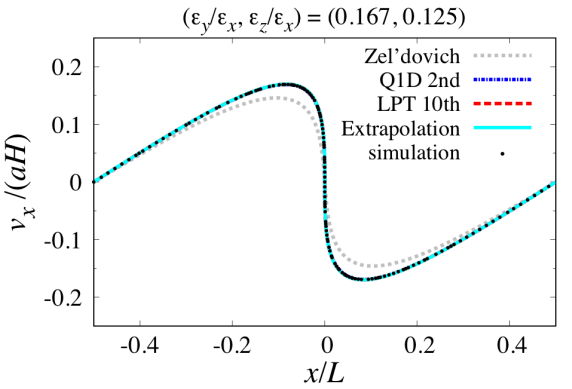

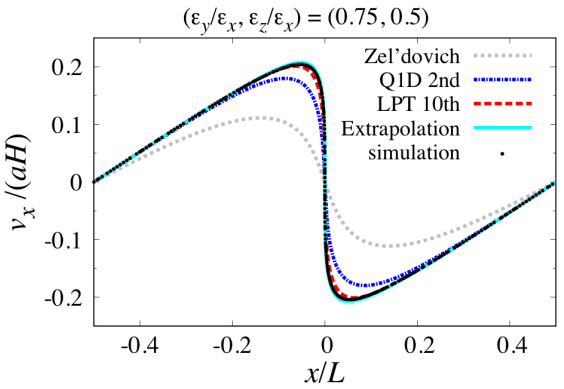

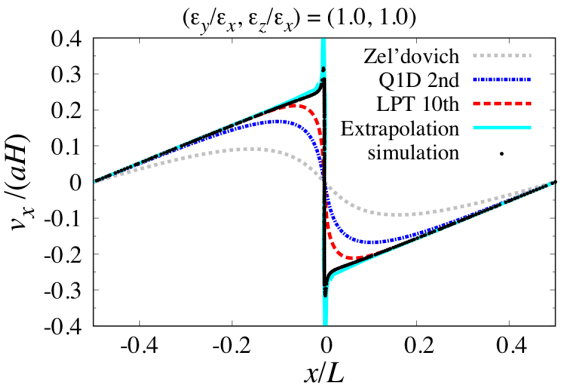

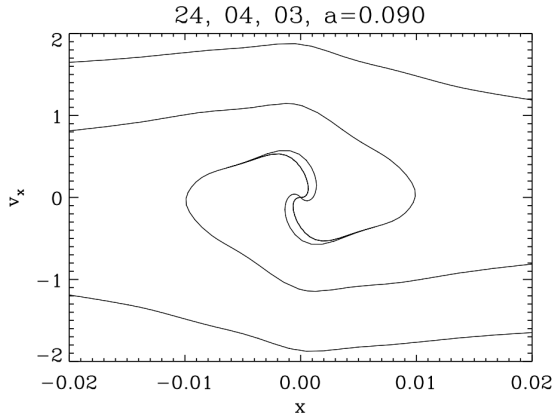

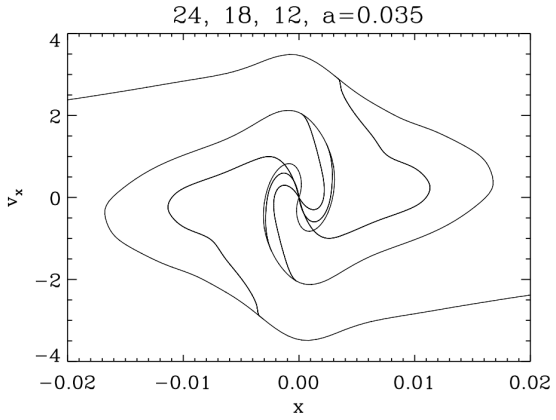

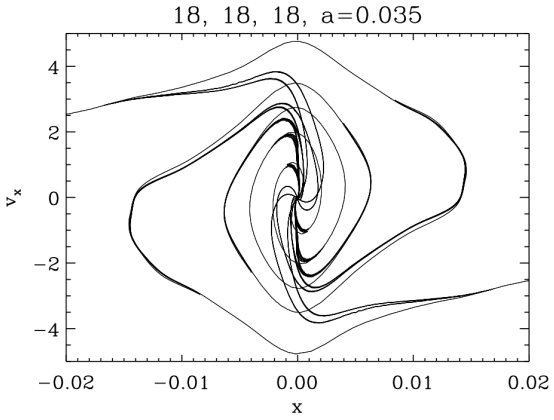

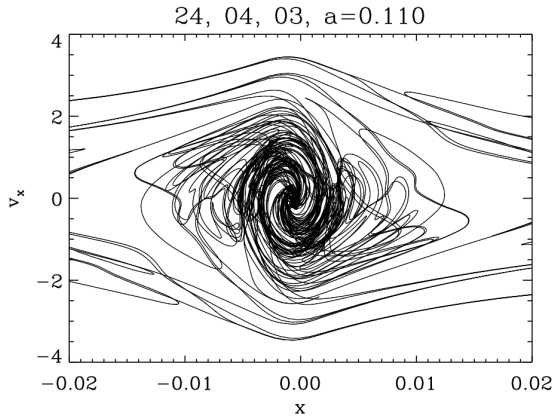

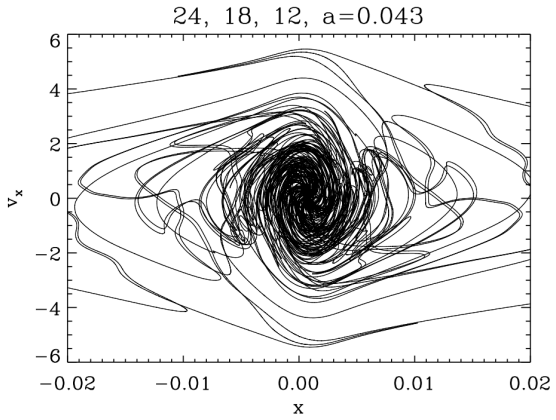

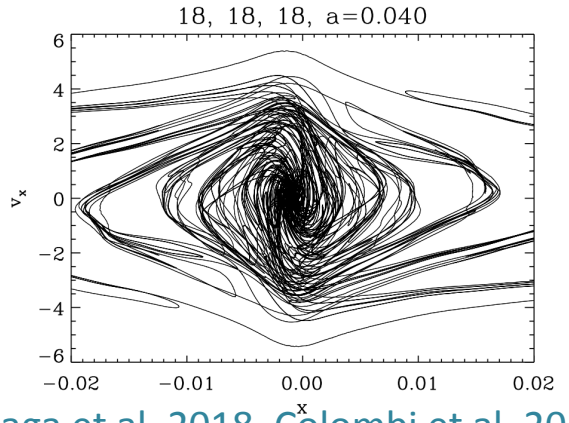

Saga et al. 2018, Colombi et al. 2018

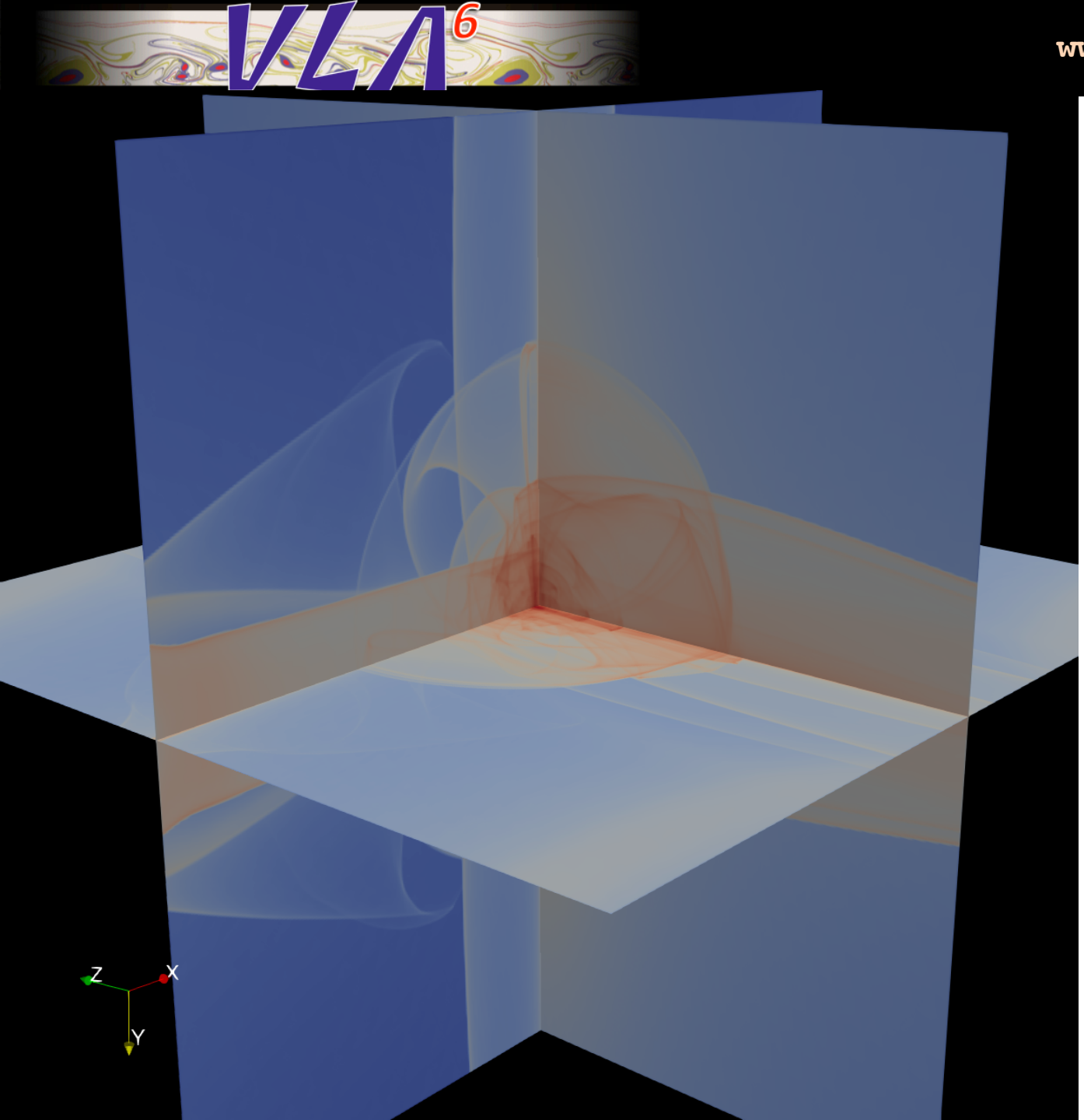

Quasi 1D case: late times

$(\varepsilon_x, \varepsilon_y, \varepsilon_z)=(-24,\ -4,\ -3)$

Colombi et al. 2018

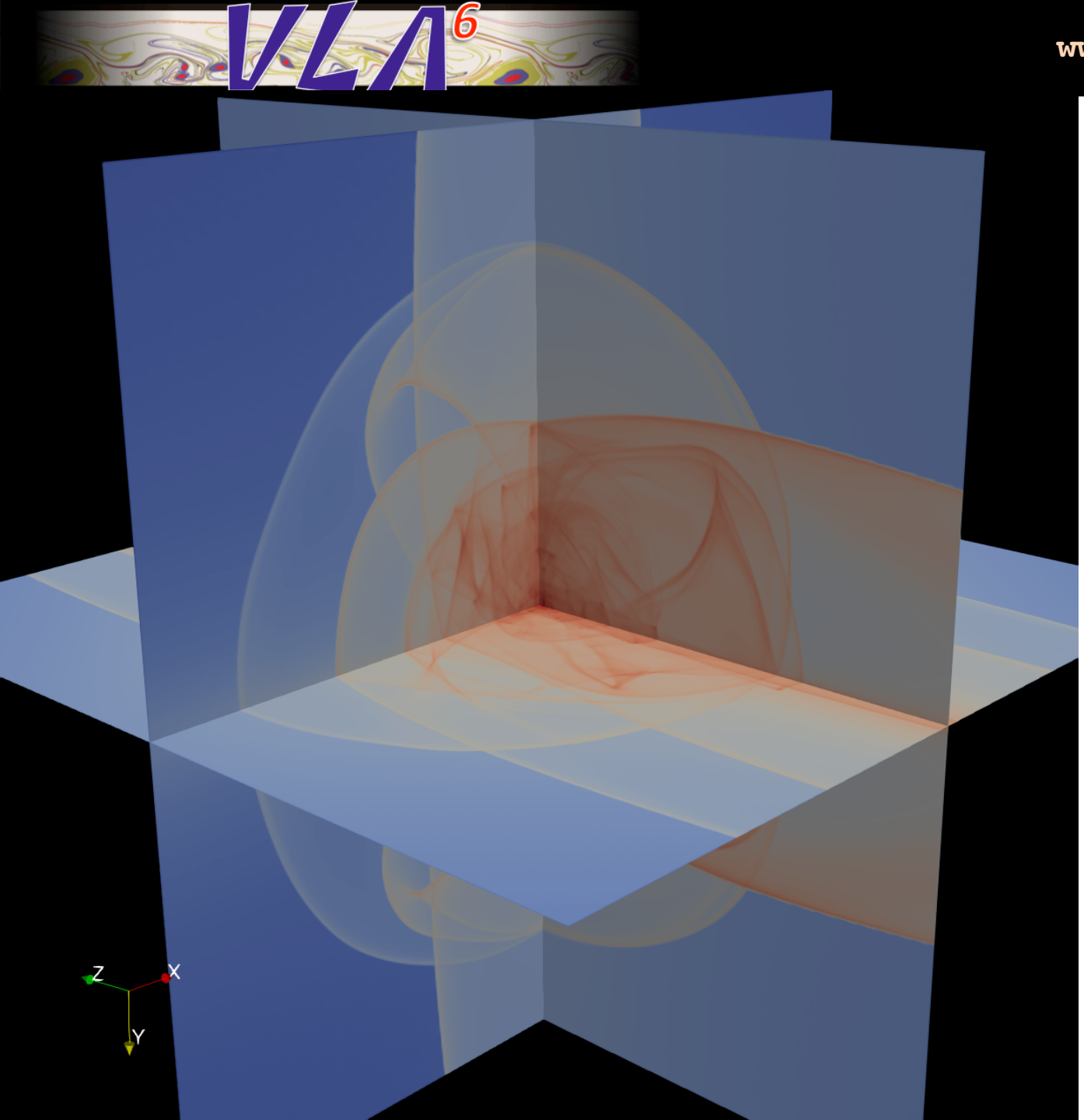

"Typical" case: late times

$(\varepsilon_x, \varepsilon_y, \varepsilon_z)=(-24,\ -18,\ -12)$

Colombi et al. 2018

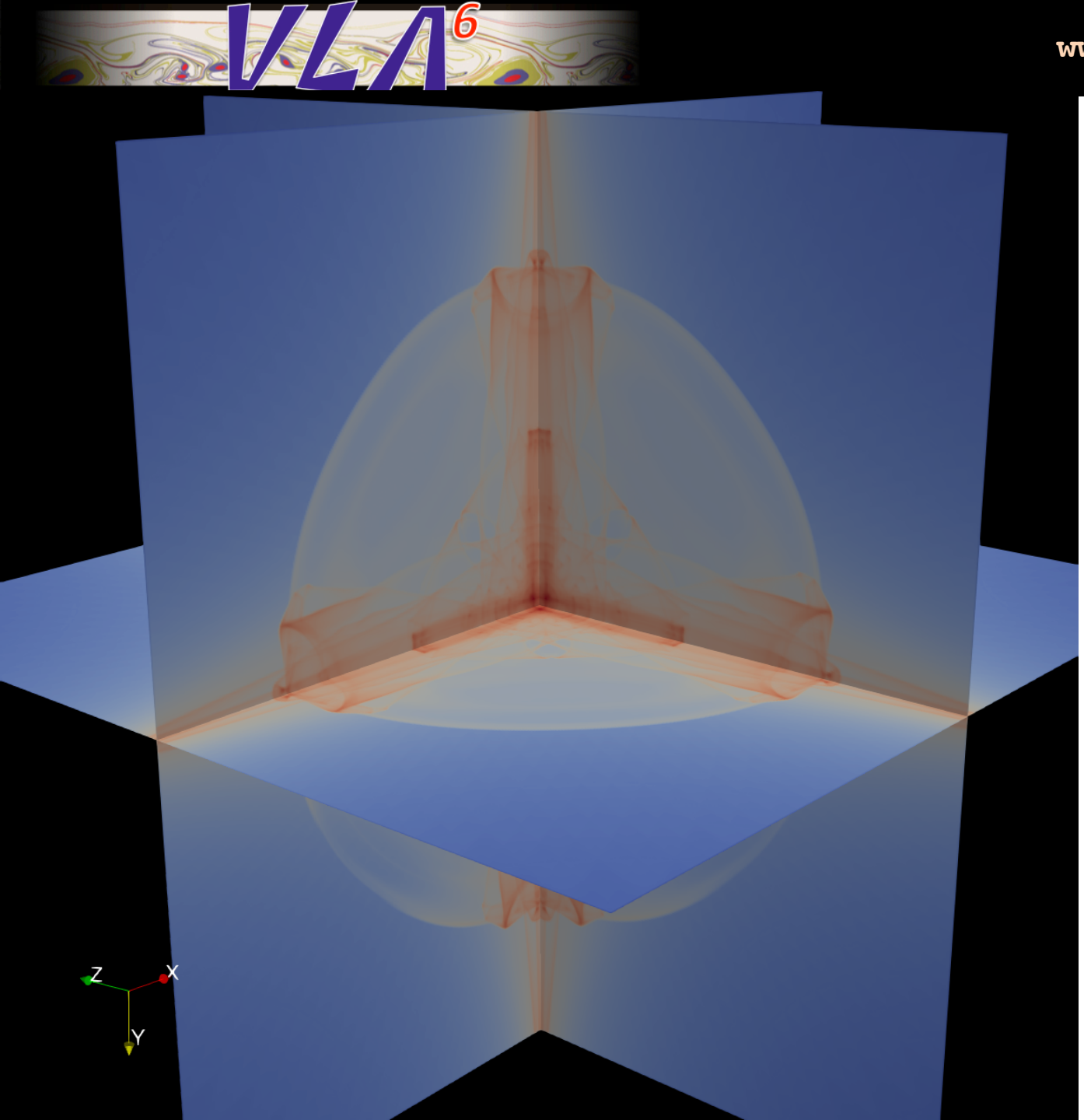

Triaxial symmetric case: late times

$(\varepsilon_x, \varepsilon_y, \varepsilon_z)=(-18,\ -18,\ -18)$

Colombi et al. 2018

A few words about the runs

Main runs on 3072 cores of Occigen (CINES) (about 90Tb data generated)

	Amplitudes	Shift	N_g	N_s	ϵ_I	CPU (heures)	n_s
(a)	24, 18, 12		512	256	10^{-6}	70200	2.90×10^9
(b)	"	✓	512	256	10^{-6}	70400	3.51×10^9
(c)	"		512	512	10^{-7}	306500	10.4×10^9
(d)	18, 18, 18		512	256	10^{-6}	70150	7.59×10^9
(e)	"	✓	512	256	10^{-6}	82000	10.4×10^9
(f)	24, 21, 12	✓	512	256	10^{-6}	87100	5.92×10^9
(g)	24, 15, 12	✓	512	256	10^{-6}	87100	4.39×10^9
(h)	18, 18, 18		512	512	10^{-7}	358000	9.57×10^9
(i)	24, 18, 12		1024	512	10^{-7}	188500	8.05×10^8
(j)	24, 21, 12		512	512	10^{-7}	69900	1.95×10^9
(k)	24, 15, 12		512	512	10^{-7}	69800	1.63×10^9
(l)	24, 04, 03		512	256	10^{-6}	74300	1.96×10^9

Extract from a DARI report by S. Colombi

TABLE 1 – Paramètres des plus grosses simulations, réalisées sur 3072 cœurs de la machine Occigen, et dont les conditions initiales correspondent à trois ondes sinusoïdales orthogonales dans une boîte périodique. Les amplitudes respectives des trois ondes sont données dans la première colonne. La colonne "shift" indique si un décalage d'une demi-cellule de la grille utilisée pour calculer la force a été réalisé dans les conditions initiales : cela change les propriétés de symétrie locale de la nappe dans l'espace des phases. La quantité N_g correspond à la résolution de la grille utilisée pour résoudre l'équation de Poisson tandis que N_s donne la résolution du réseau initial pour construire la tessellation correspondant à la nappe dans l'espace des phases. Le paramètre ϵ_I donne la valeur de la contrainte de raffinement sur les invariants de Poincaré. Finalement, les deux dernières colonnes donnent le temps de calcul total consommé par chaque simulation et le nombre final n_s de simplex à la fin du run. La double-ligne horizontale au milieu de la table sépare les simulations réalisées en 2016 (au dessus de la double-ligne) de celles réalisées en 2017 (en dessous de la double-ligne).

Post analysis performed on Horizon cluster of IAP

Post-collapse peturbation theory

Colombi 2015, MNRAS 446, 2902
Taruya & Colombi 2017, MNRAS 470, 4858

- The main idea is that at collapse time the system presents a quasi-1D structure.

- In 1D dynamics, linear Lagrangian perturbation theory provides exact solution prior to collapse time. It can be used as a first approximation of the dynamics just after collapse time.

$$x(Q;\tau) = x_{\rm Zel}(Q;\tau) \equiv q + \psi(q) D_+(\tau),$$
$$u(Q;\tau) = u_{\rm Zel}(Q;\tau) \equiv \psi(q) \frac{{\rm d}D_+(\tau)}{{\rm d}\tau}.$$

- Correction to the force, hence to the motion, is computed just after collapse time assuming that *x(Q)* and *v(Q)* are third order polynomials of Lagrangian position *Q*, which is correct asymptotically.

$$x(Q;\tau) = x_{\rm Zel}(Q;\,\widehat{\tau}_{\rm c}(Q)) + \Delta x_{\rm out}(Q;\tau,\,\widehat{\tau}_{\rm c}(Q)),$$
$$u(Q;\tau) = u_{\rm Zel}(Q;\,\widehat{\tau}_{\rm c}(Q)) + \Delta u_{\rm out}(Q;\tau,\,\widehat{\tau}_{\rm c}(Q)).$$

- Generalization to higher number of dimensions requires an accurate prediction of the system at collapse time, but should be analogous to the 1D calculations if quasi 1D regime is valid

- Current investigations (with A. Taruya & S. Saga):
- Higher order Lagrangian perturbation theory (following footsteps of Moutarde et al. 1991)
- Higher order Lagrangian perturbation theory in the quasi-1D framework (following footsteps of Rampf & Frisch 2017)

Collapse occurs at peaks of the initial density: $\delta_{\rm L}(q_0) = \dfrac{1}{D_+(\tau_0)}, \quad \left.\dfrac{{\rm d}\delta_{\rm L}(q)}{{\rm d}q}\right|_{q_0} = 0, \quad \left.\dfrac{{\rm d}^2\delta_{\rm L}(q)}{{\rm d}q^2}\right|_{q_0} < 0.$

At collapse the motion can be locally expanded at third order in the Lagrangian coordinate

$$x(q;\tau) \simeq A(q_0;\tau) - B(q_0;\tau)\,(q-q_0) + C(q_0;\tau)\,(q-q_0)^3$$

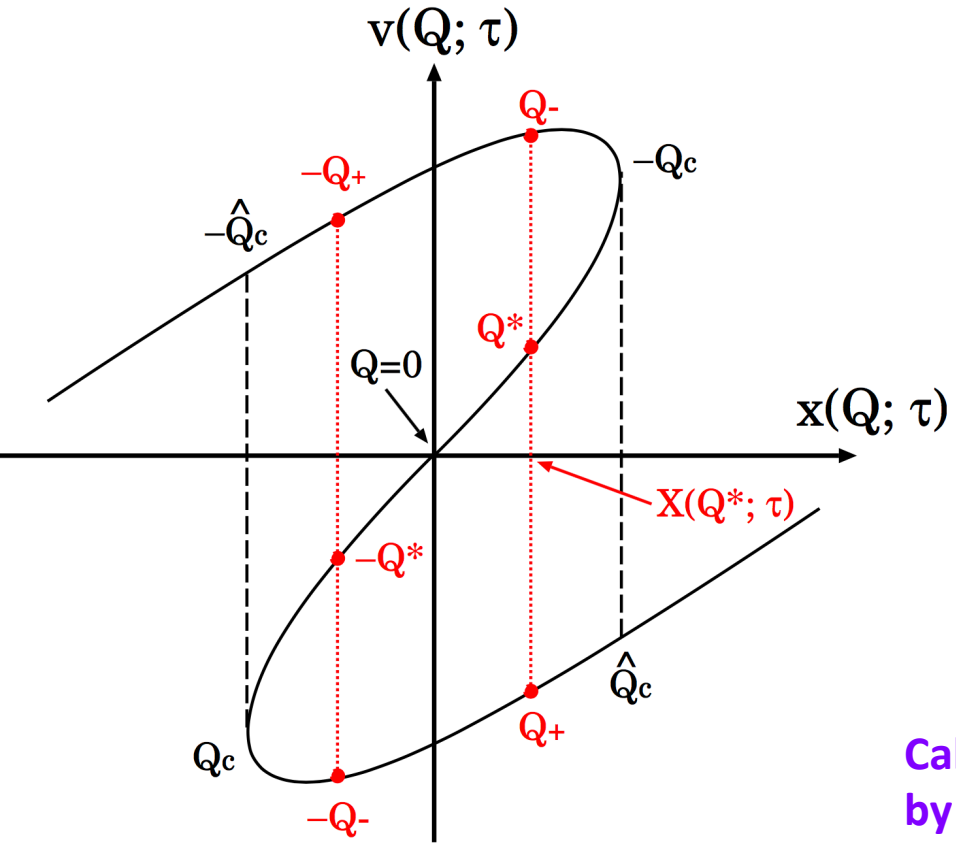

$$A(q_0;\tau) \equiv x(q_0;\tau) = q_0 + D_+(\tau)\,\psi(q_0),$$

$$B(q_0;\tau) \equiv -\left.\frac{\partial x}{\partial q}\right|_{q_0} = -1 - D_+(\tau)\psi'(q_0) = \{D_+(\tau) - D_+(\tau_0)\}\,\delta_{\rm L}(q_0),$$

$$C(q_0;\tau) \equiv \frac{1}{6}\left.\frac{\partial^3 x}{\partial q^3}\right|_{q_0} = \frac{1}{6}\,D_+(\tau)\,\psi'''(q_0) = -\frac{1}{6}\,D_+(\tau)\,\delta_{\rm L}''(q_0),$$

Calculation of the acceleration is then facilitated by the fact that the multivalued equation *x(Q)=x(Q')* has simple solutions

Example: collapse of a single sine wave

Taruya & Colombi 2017, MNRAS 470, 4858